How Much Is the Smirk Worth? Downside Risk Pricing in Cattle Options

Esteban Vizcarrondo, Teresa Serra, and Andrew McKenzie

Suggested citation format:

Vizcarrondo, E., Serra, T., and McKenzie, A. 2026. “How Much Is the Smirk Worth? Downside Risk Pricing in Cattle Options.” Proceedings of the NCCC-134 Conference on Applied Commodity Price Analysis, Forecasting, and Market Risk Management, Chicago, Illinois, April 20-21, 2026. [http://www.farmdoc.illinois.edu/nccc134/paperarchive]

How Much Is the Smirk Worth? Downside Risk Pricing in Cattle Options*

Esteban Vizcarrondo† Teresa Serra‡ Andrew McKenzie §

Paper prepared for the NCCC-134 Conference on Applied Commodity Price Analysis, Forecasting, and Market Risk Management, 2026.

*This work was supported by the Bielfeldt Office for Futures and Options Research at the University of Illinois. We thank participants in the Food, Agriculture, and Commodities Seminar at the Department of Agricultural and Consumer Economics for their helpful comments. We especially thank Hang Lin and Richie Ma for thoughtful conversations.

†Corresponding Author. PhD Student. University of Illinois at Urbana-Champaign. Email: ejv3@illinois.edu

‡Hieronymous Distinguished Chair. Professor. University of Illinois at Urbana-Champaign. Email: tserra@illinois.edu

§Fryar Endowed Chair. Professor. University of Arkansas. Email: mckenzie@uark.edu

How Much Is the Smirk Worth? Downside Risk Pricing in Cattle Options

Abstract

We develop a daily leverage premium measuring downside-asymmetric volatility risk within the filtered historical simulation framework of Barone-Adesi, Engle, and Mancini (2008). The leverage premium isolates the component of option-implied expected variance attributable to downside asymmetry beyond historical volatility dynamics. Applying this framework to daily options on live cattle, feeder cattle, and corn over 2019, we find that cattle options price about 25% more expected variance for downside asymmetry than historical patterns would justify—roughly twice the corn level. We then exploit the August 9, 2019 Tyson Holcomb fire to test whether option markets reprice downside risk following severe supply-chain disruptions. Using a difference-in-differences design with corn as the control market, the leverage premium increases for live cattle options during the disruption—by approximately 14% for regular options and 23% for serial options—and attenuates as processing capacity is restored. Feeder cattle, which are further upstream from the processing bottleneck, show no comparable response. Translated into hedging costs via a local Black (1976) approximation, the repricing implies \$1.60–1.90 per head in additional cost for a representative short-dated, out-of-the-money live cattle put.

Keywords: agricultural options, downside risk, GARCH option pricing, variance risk premium

JEL Codes: G1; Q1

1 Introduction

Cattle producers and feedlots face a distinctive form of production risk because market-ready animals must be processed within a relatively narrow window. Once cattle reach market weight, delays in slaughter can generate quality losses, added feeding costs, and marketing difficulties that reduce their value. This leaves cattle market participants with limited ability to smooth adverse shocks through storage or postponed sale. The contrast with grain is important. Grain producers can often carry inventory and wait for better market conditions, whereas cattle producers have more limited flexibility once animals reach market weight. As a result, they are especially exposed when processing capacity becomes constrained. If a major packing plant goes offline—because of fire, disease outbreak, or another disruption—cattle can accumulate at feedlots, leading to delayed marketings and discounted sales. The August 2019 fire at Tyson's Holcomb, Kansas facility, which eliminated roughly 6% of U.S. beef-processing capacity and resulted in a 9% drop in live cattle futures prices over the week following the fire, illustrates how concentrated processing infrastructure can generate downside risk that cannot be readily smoothed through inventory management (Dennis, 2020; USDA AMS, 2020). The facility partially resumed operations in November 2019 and returned to near-full capacity by late December 2019. These disruptions are especially relevant for derivative markets because they expose producers to sharp downside price risk over relatively short horizons.

Options provide a natural way to study downside risk because their prices reflect both the expected price volatility and market compensation required for downside protection. Out-of-the-money (OTM) put options are especially informative because they pay off only when prices fall sharply, directly reflecting perceived downside risk. In live and feeder cattle options, these contracts trade at higher implied volatilities than comparable calls, producing a pronounced leftward implied-volatility smirk relative to the constant-volatility benchmarks of Black (1976). McKenzie, Thomsen, and Adjemian (2022) document this pattern and interpret it as evidence of persistent demand for crash protection by cattle producers. Thomsen, McKenzie, and Power (2013) further show that deep OTM puts partially anticipated the 2003 BSE outbreak. Figure 1 illustrates this asymmetry around the Holcomb fire, with each panel comparing implied volatility over matched windows before

Figure 1: Live Cattle Implied Volatility Smirk Around the Holcomb Fire

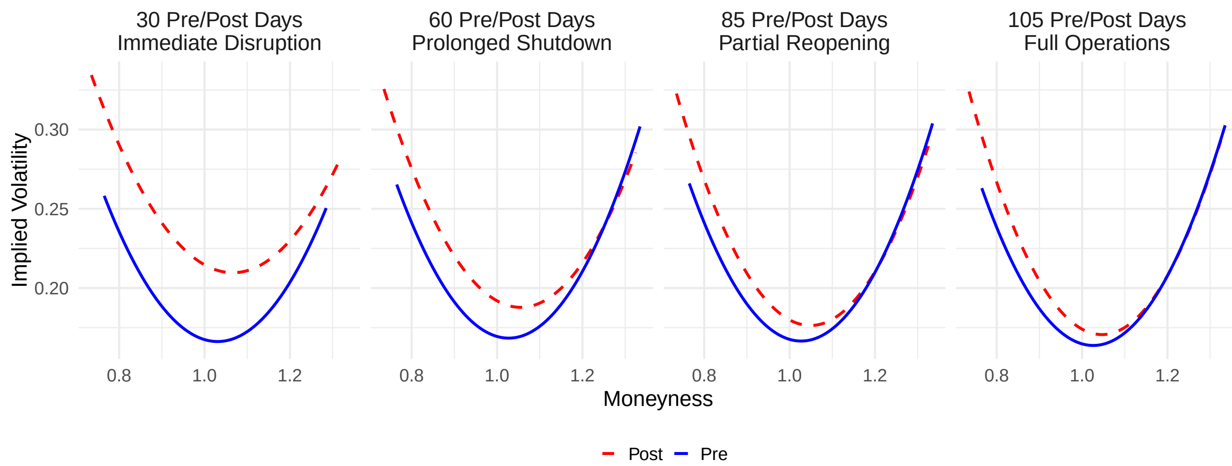

Note: Implied volatility before and after the Tyson Holcomb fire for live cattle regular OTM options. Each panel displays second-degree polynomial fits of mean implied volatility against moneyness for pre-event (solid) and post-event (dashed) windows of varying length. Window labels correspond to capacity milestones from Dennis (2020). The post-fire shift is concentrated on the OTM put side (moneyness < 1), consistent with increased demand for downside protection. The gap narrows as capacity is restored.

and after the event, showing a pronounced steepening of the smirk for live cattle.

While prior research documents persistent downside asymmetry in livestock option markets, it does not construct a time-varying measure of the compensation embedded in option prices for bearing downside volatility risk. We focus on a risk premium rather than a skew statistic. The implied-volatility skew describes the shape of the pricing surface, whereas a risk premium quantifies the compensation market participants require for bearing a particular risk exposure. Following the logic of variance risk premia in Carr and Wu (2009), we isolate the component of option-implied variance associated with downside-asymmetric risk and refer to it as the leverage premium.

To construct this measure, we use the filtered historical simulation (FHS) framework of Barone-Adesi, Engle, and Mancini (2008), which separately estimates physical volatility dynamics from futures returns and risk-neutral dynamics from option prices. The leverage premium is then constructed by comparing option-implied expected variance with a counterfactual benchmark that preserves historical downside asymmetry. The resulting wedge provides a measure of priced downside risk that can be tracked at daily frequency.

We estimate the measure daily for live cattle, feeder cattle, and corn options surrounding the August 2019 Holcomb fire. Using a difference-in-differences (DiD) design with corn as the control market, we find that the leverage premium rises for live cattle relative to corn during the active disruption period. In our preferred specification, with trend, microstructure, and seasonality controls, the log leverage premium increases by approximately 14% for regular options and 23% for serial options over the 72 business days between the fire and partial plant reopening.

Specifications that further include CFTC commercial hedging-pressure controls raise the regular-options estimate to 27–29%, suggesting that commercial positioning partially masks the underlying repricing in specifications that omit hedging controls. The effect attenuates as processing capacity is restored, declining toward zero in wider windows that encompass the full reopening—consistent with option markets pricing a transitory downside shock rather than a permanent reassessment of risk. Feeder cattle options, by contrast, show no evidence of a positive shift, supporting the interpretation that the repricing was concentrated in the market most directly exposed to the processing bottleneck. Translated into hedging costs via a local Black (1976) approximation, the repricing implies roughly \$1.60–1.90 per head in additional put-option cost, a meaningful increment given that feedyard margins were near breakeven during the shutdown period.

This paper contributes to the literature on agricultural options pricing by constructing a time-varying measure of priced downside-asymmetric volatility risk in livestock options markets and using it to study how option markets respond to a realized supply-chain disruption. Prior research documents pronounced leftward skews in livestock options markets (Turvey and Komar, 2007; Bozic and Fortenbery, 2010; Thomsen and McKenzie, 2010; McKenzie et al., 2022) and provides some evidence that deep OTM puts may reflect expectations about rare livestock shocks (Thomsen, McKenzie, and Power, 2013). However, this literature does not provide a time-varying measure of the compensation markets require for bearing downside volatility risk. Applying the measure to daily options on live cattle, feeder cattle, and corn over 2019, we find that cattle options price about 25% more expected variance for downside asymmetry than historical patterns would justify—roughly twice the corn level. By constructing such a measure within the FHS framework and examining its response to the Tyson Holcomb disruption using a DiD design supplemented by permutation inference, this paper provides evidence that option markets reprice downside protection after a realized processing shock, and that the repricing dissipates as the underlying supply disruption is resolved. More broadly, the paper contributes to the literature debating whether livestock option smirks primarily reflect fundamental downside-risk pricing or commercial hedging pressure. We show that the leverage premium responds to an exogenous processing disruption and remains positive after controlling for hedging activity, consistent with livestock option smirks partly reflecting fundamental downside-risk pricing in addition to commercial hedging pressure.

The paper proceeds as follows. Section 2 details the methodology and leverage premium construction. Section 3 describes the data and estimation. Section 4 presents the DiD identification strategy and results. Section 5 concludes.

2 Methodology

Our empirical strategy exploits the distinction between how volatility has historically behaved and how markets price it today. Physical (P) dynamics, estimated from past returns, describe the historical evolution of volatility. Risk-neutral (Q) dynamics, inferred from option prices, describe the risk-neutral distribution used for valuation. Our leverage premium targets the component of this wedge attributable to asymmetric downside volatility. We first estimate the physical dynamics from returns, then infer risk-neutral dynamics from option prices, and finally construct the leverage premium from the difference between Q and a counterfactual that holds asymmetry fixed at its historical level.

2.1 Physical Dynamics

We model log futures returns under the physical measure P using the GJR-GARCH(1,1) specification of Glosten, Jagannathan, and Runkle (1993):

$$\log\left(\frac{F_t}{F_{t-1}}\right) = \mu + \varepsilon_t, \tag{1}$$

$$\sigma_{t+1}^2 = \omega + \beta\sigma_t^2 + \alpha\varepsilon_t^2 + \gamma I_t \varepsilon_t^2, \tag{2}$$

where F_t is the nearby futures price, $\varepsilon_t = \sigma_t z_t$, and $z_t \sim f(0,1)$ are i.i.d. standardized innovations drawn from the empirical distribution of historical residuals. The indicator $I_t = \mathbf{1}(\varepsilon_t < 0)$ captures negative return shocks. The parameter γ governs asymmetric volatility response to negative shocks; when $\gamma > 0$ bad news increases conditional variance more than good news of equal magnitude.

Physical parameters $\theta = \{\mu, \omega, \beta, \alpha, \gamma\}$ are estimated via pseudo-maximum likelihood on a rolling 3,500-day window of daily futures returns, allowing the physical volatility parameters to update over time and produce daily estimates. Stationarity requires $\beta + \alpha + \lambda\gamma < 1$, where $\lambda \equiv E[z^2\mathbf{1}(z < 0)]$ is computed from the empirical distribution (and equals 1/2 under symmetry).

2.2 Risk-Neutral Calibration

Because volatility cannot be fully hedged using traded assets, risk-neutral dynamics cannot be recovered from futures returns alone and are instead inferred from option prices. Our question requires separating historical volatility dynamics from the market's pricing of downside asymmetry; FHS makes this separation operational by estimating P-dynamics from returns and inferring Q-dynamics from option prices. We calibrate risk-neutral parameters $\theta^* = \{\omega^*, \beta^*, \alpha^*, \gamma^*\}$ daily by minimizing squared pricing errors across the N_t option contracts on date t:

$$\theta^* = \arg\min_{\theta^*} \sum_{j=1}^{N_t} [\text{Model Price}_j(\theta^*) - \text{Market Price}_j]^2 \tag{3}$$

subject to $\omega^* > 0$, $\alpha^*, \beta^*, \gamma^* \geq 0$, and $\beta^* + \alpha^* + \lambda\gamma^* < 1$.

Model prices are computed via FHS following Barone-Adesi, Engle, and Mancini (2008). For each candidate θ^*, we simulate 20,000 price paths by drawing innovations with replacement from the empirical residual distribution and updating conditional variance using θ^*. The futures price must be a martingale under Q; we enforce this restriction via empirical martingale simulation (Duan and Simonato, 1998) and compute option values as discounted expected payoffs at the risk-free rate (see Appendix A for full implementation details). The martingale restriction has a simple interpretation: under risk-neutral pricing, the futures price has no systematic drift, so today's futures price equals the risk-neutral expectation of tomorrow's price.

We calibrate to OTM options with more than 14 business days to expiration (Barone-Adesi et al., 2008; Dumas, Fleming, and Whaley, 1998). Shorter-maturity contracts are excluded because their time value decays at an accelerating rate near expiration, leaving prices that reflect imminent realized rather than forward-looking variance. For regular options, on each date we first identify the nearby futures contract and its remaining life to expiration, then retain OTM options whose expirations map to that nearby contract. Hence, for regular options, the longest maturity in the calibration sample is the time left until the nearby futures expires, which varies by commodity. For serial options, expirations follow the option-specific monthly serial calendar (including non-standard months), not the regular options cycle tied to nearby futures contract months. See Table B.1 in Appendix B for further details on futures-options expiry schedule.

2.3 Leverage Premium Construction

This section constructs a measure of how option markets price downside risk relative to historical volatility dynamics. Our key object is the wedge between option-implied and historical assessments of downside risk. Define realized variance over horizon τ as $RV_{t,T} = \frac{1}{\tau}\sum_{i=t+1}^{T}\sigma_i^2$, where $T = t+\tau$. Following Carr and Wu (2009), define the variance risk premium as:

$$VRP_{t,T} = E^Q[RV_{t,T} \mid \mathcal{F}_t] - E^P[RV_{t,T} \mid \mathcal{F}_t], \tag{4}$$

where $\mathcal{F}_t$ denotes the time-t information set, including the updated conditional variance σ_{t+1}^2 which is known at time t as the one-step-ahead conditional variance. Positive values indicate that option-implied expected variance exceeds historical expected variance.

To isolate the contribution of asymmetric volatility pricing, we construct a counterfactual measure $\tilde{Q}$ with parameters $(\omega^*, \beta^*, \alpha^*, \gamma)$—adopting option-implied base dynamics while retaining the historical asymmetry parameter. The leverage component of the VRP is:

$$VRP_{t,T}^{leverage} = E^Q[RV_{t,T} \mid \mathcal{F}_t] - E^{\tilde{Q}}[RV_{t,T} \mid \mathcal{F}_t]. \tag{5}$$

This measures how much option-implied expected variance increases when markets price asymmetric volatility (γ^*) differently than what historical patterns suggest (γ).

Under GJR-GARCH, expected realized variance admits a closed form (see Appendix A for derivation and implementation details). For any measure $J \in \{P, \tilde{Q}, Q\}$ with effective persistence $\phi^J = \beta^J + \alpha^J + \lambda\gamma^J$ (using the same $\lambda \equiv E[z^2\mathbf{1}(z < 0)]$ from the empirical distribution), and with horizons expressed in trading-year units using the standard 252-trading-day convention:

$$E^J[RV_{t,T} \mid \mathcal{F}_t] = \bar{\sigma}^{2,J}(1 - \kappa_\tau^J) + \sigma_{t+1}^2\kappa_\tau^J, \tag{6}$$

where $\bar{\sigma}^{2,J} = \omega^J/(1 - \phi^J)$ and $\kappa_\tau^J = \frac{1-(\phi^J)^\tau}{\tau(1-\phi^J)}$.

Our primary dependent variable is the log leverage premium:

$$\text{Log Leverage Premium}_{t,T} = \log\left(\frac{E^Q[RV_{t,T} \mid \mathcal{F}_t]}{E^{\tilde{Q}}[RV_{t,T} \mid \mathcal{F}_t]}\right). \tag{7}$$

This captures the percentage increase in option-implied expected variance attributable to priced asymmetry beyond historical levels, and can be computed daily. Because the risk-neutral calibration aggregates information across the option cross-section on each date, the resulting leverage premium is a single daily measure for each commodity.

3 Data and Estimation

This section describes the data, sample construction, and model estimates. We first describe the data used to implement the FHS framework, then report physical and risk-neutral parameter estimates, and finally present the variance risk premium decomposition used in the event study.

3.1 Data Sources and Sample Construction

Our analysis combines futures and options data for three commodities: live cattle, feeder cattle, and corn, with feeder cattle providing an upstream comparison market that is less exposed to processing capacity constraints and corn serving as the control market in the DiD analysis. We obtain daily settlement futures prices from Bloomberg, the nearby price series is computed using a 15-day calendar roll, whereby positions are rolled into the next contract 15 calendar days prior to expiration. Options data come from Barchart, which provides daily settlement prices, implied volatilities (IVs), and contract specifications for CME-listed agricultural options. Our sample spans January 31, 2019 through February 14, 2020, comprising 136 business days before and 136 after the August 9, 2019 event. We end the sample before the onset of COVID-19 market disruptions, which independently affected meatpacking operations beginning in late February 2020. To isolate the active disruption period, we also estimate specifications using narrower symmetric windows of 72 business days (fire to partial reopening) and 107 business days (fire to full reopening), based on capacity restoration milestones documented in Dennis (2020).

We match options to their underlying futures contracts and impose filters following Barone-Adesi et al. (2008). We exclude options with implied volatilities exceeding 70% or settlement prices below \$0.05 to remove illiquid or potentially mispriced contracts that may introduce noise into the calibration. Regular option expirations differ by commodity: live cattle options expire in even months; feeder cattle options in January, March, April, May, August, September, October, and November; and corn options expire in delivery months (March, May, July, September, December).[1] Serial options fill the intervening months, though they are not listed by CME for feeder cattle contracts. Serial options typically have shorter maturities, reducing cross-sectional heterogeneity in the calibration sample and improving model fit (see section 3.2); regular options span longer horizons where persistence effects accumulate.

Table 1 reports summary statistics for regular and serial OTM options, stratified by moneyness ranges, over the event-study sample from January 2019 to February 2020. Deep OTM puts ($K/F < 0.85$) command higher implied volatilities than near-the-money puts for both live cattle and feeder cattle contracts. For live cattle regular options, the spread is approximately 6 percentage points (23.98% vs. 18.41%); for feeder cattle, the gap is about 5 percentage points (21.14% vs. 16.19%). This pattern reflects the curvature of the implied volatility surface.

In our sample, trading activity concentrates in near-the-money options. For corn regular options, near-the-money puts and calls account for over 3.1 million and 4.9 million contracts traded over the sample period, respectively, compared to roughly 108,000 and 1.0 million for deep OTM options. Cattle regular options are substantially less liquid, with live cattle volumes roughly one-tenth of corn's. Feeder cattle regular option volume is roughly one-tenth of live cattle's.

[1]For further details on futures and options expiry rules see Table B.1 in Appendix B.

Across both regular and serial contracts, cattle option implied volatility shows a clear downside premium relative to corn, with OTM puts carrying higher IV than comparable OTM calls. This pattern is pronounced in deep out-of-the-money contracts. In regular options, the deep-OTM put–call IV gap is 2.80 percentage points in live cattle (i.e., 23.98% vs. 21.18%) and 1.07 percentage points in feeder cattle, whereas corn exhibits a negative gap of -1.85 percentage points. In serial options, live cattle shows a similar pattern, with a put premium of 3.70 percentage points, while corn displays again a negative gap of -1.41 percentage points. More broadly, across moneyness ranges, OTM cattle puts consistently trade at higher implied volatilities than calls, in contrast to corn where the pattern is reversed. These differences indicate a consistent volatility smirk in cattle options and systematically stronger pricing of downside risk relative to corn.

In price terms, the asymmetry is less pronounced for deep OTM contracts in cattle options, where both puts and calls are priced close to zero (e.g., \$0.08 in live cattle for regular options). Nevertheless, OTM cattle options exhibit higher put prices relative to comparable calls (e.g., \$0.77 for puts vs. \$0.75 for calls for regular options), consistent with stronger demand for downside protection. For corn, call premia remain higher in dollar terms.

Because the GJR term γ is the model's main channel for capturing downside-asymmetric volatility, we expect the specification to fit best in markets where the option surface exhibits a pronounced leftward smirk. In our sample, cattle options display systematically higher implied volatility for OTM puts than for comparable calls, whereas corn appears comparatively flatter. Ex ante, this suggests that the asymmetric component should be more important for live and feeder cattle than for corn. To the extent that volatility adjusts symmetrically, that response should instead be absorbed by α, with γ contributing relatively less to corn when compared to the cattle contracts. In the empirical implementation, each daily calibration uses an average of about 40 option contracts per commodity, though the cross section thins to about 20 contracts as observations approach the 14-day maturity cutoff.

Table 1: Summary Statistics for Regular and Serial Options

K/F	Type	Price $	Std.dev	σ_{B76} %	Std.dev	Volume	Obs
Panel A: Regular Options							
Corn							
< 0.85	Put	0.18	0.20	39.26	13.48	107,534	4,355
[0.85, 1.00)	Put	3.68	4.59	20.97	6.38	3,120,636	2,884
(1.00, 1.15]	Call	5.50	5.18	24.56	8.18	4,870,573	2,899
> 1.15	Call	0.64	1.25	41.11	11.89	1,022,547	7,547
Feeder Cattle							
< 0.85	Put	0.08	0.05	21.14	3.74	212	545
[0.85, 1.00)	Put	0.99	0.99	16.19	3.60	59,363	6,046
(1.00, 1.15]	Call	0.98	0.98	14.91	3.25	50,804	5,843
> 1.15	Call	0.12	0.08	20.07	3.82	2,808	1,017
Live Cattle							
< 0.85	Put	0.08	0.05	23.98	3.40	2,996	721
[0.85, 1.00)	Put	0.77	0.79	18.41	3.26	451,549	4,188
(1.00, 1.15]	Call	0.75	0.77	16.39	2.56	364,655	3,965
> 1.15	Call	0.08	0.04	21.18	2.83	8,873	1,105
Panel B: Serial Options							
Corn							
< 0.85	Put	0.19	0.22	33.88	10.08	39,034	2,794
[0.85, 1.00)	Put	3.40	4.50	20.92	6.29	1,394,340	3,058
(1.00, 1.15]	Call	4.96	5.17	23.88	7.96	2,024,339	3,070
> 1.15	Call	0.88	1.47	35.29	9.48	260,370	3,754
Live Cattle							
< 0.85	Put	0.07	0.04	29.35	8.46	2	261
[0.85, 1.00)	Put	0.65	0.67	18.45	3.74	44,348	2,835
(1.00, 1.15]	Call	0.61	0.66	16.44	2.72	43,874	2,769
> 1.15	Call	0.07	0.04	25.65	6.26	13	372

Note: The tables report summary statistics for standard regular and serial OTM options on agricultural futures from January 31, 2019 to February 14, 2020. For each trading day, we select the closest standard option expiry with more than 14 business days to expiration, ensuring a single maturity per day. Regular options (Panel A) are identified by their expiration alignment with futures contract cycles: Live Cattle options expire the first Thursday/Friday of even months, Feeder Cattle the last Thursday of contract months (Jan, Mar, Apr, May, Aug, Sep, Oct, Nov), and Corn the last Friday before delivery months (Mar, May, Jul, Sep, Dec). Panel B includes serial options (CME does not list options for feeder cattle). Options are filtered to exclude implied volatilities above $\geq 70\%$ and settlement prices below($\leq$ \$0.05). For each commodity and moneyness range (strike-to-underlying ratio, K/F), the table reports the average option price (USD), the standard deviation of prices, the average Black-76 implied volatility (%), its standard deviation, total volume, and the number of observations (strike-date-expiration combinations with settlement prices). Moneyness ranges are defined separately for puts ($K/F < 1$) and calls ($K/F > 1$) and include only OTM options.

3.2 Physical and Risk-Neutral Parameter Estimates

Table 2 reports GJR-GARCH parameter estimates for regular and serial options. Panel A presents physical (P) parameters estimated from futures returns; Panel B presents risk-neutral (Q) parameters calibrated from option prices; Panel C reports model fit statistics.[2] Appendix A provides the full derivation of the leverage-premium decomposition and the filtered historical simulation algorithm used in estimation. Physical volatility persistence is high across all commodities, with persistence parameters ranging from 0.9928 (feeder cattle) to 0.9967 (live cattle), reflecting the slow mean-reversion characteristic of agricultural commodity volatility. The leverage parameter γ is positive for all commodities: 0.0370 for feeder cattle regular options, 0.0113 for live cattle regular options, and 0.0287 for corn, indicating asymmetric volatility responses across all markets.

The risk-neutral parameters differ markedly. The option-implied leverage parameter γ^* substantially exceeds its physical counterpart γ for all cattle specifications. For live cattle regular options, the gap is 0.2491 (i.e., the difference between $\gamma^* = 0.2604$ and $\gamma = 0.0113$), while for feeder cattle the gap is 0.2741. These gaps are the basis of our leverage premiums and are substantially larger for cattle than for corn (0.1552), indicating stronger pricing of downside asymmetry in cattle markets.

Risk-neutral persistence is substantially lower than physical persistence. For live cattle regular options, $\phi^* = 0.3561$ compared to $\phi = 0.9967$. A similar pattern holds for feeder cattle ($\phi^* = 0.3410$ vs. $\phi = 0.9928$) and corn ($\phi^* = 0.3324$ vs. $\phi = 0.9959$), indicating that option-implied variance expectations revert toward their long-run mean more rapidly than suggested by historical dynamics. Persistence differences are mainly driven by lower β^* in the risk-neutral estimates. One possible explanation is that the option cross-sections used for calibration place more weight on medium-horizon maturities, which are less sensitive to short-run variance carryover and thus consistent with faster mean reversion.

Model fit confirms that the specification performs better for serial than for regular options. For live cattle, serial options achieve lower pricing errors (RMSE = 0.0486) than regular options (RMSE = 0.1877). Corn exhibits larger pricing errors (RMSE = 0.5276 for regular and 0.3655 for

[2]See Appendix Figure B.1 for the futures contract settlement price series across January 2006 to December 2021 and Appendix Figure B.2 for a GJR-GARCH calibration exercise example.

serial options), reflecting the more complex option surface in storable commodities. The better fit for serial options is consistent with their shorter effective maturities. Over shorter horizons, option values place greater weight on near-term conditional variance, so the GJR-FHS recursion can track prices more closely. At longer maturities, which are more common in regular contracts, prices depend more on the full variance term structure and on features not captured by the model (e.g., slower-moving risk premia or contract-specific effects), which increases pricing errors. In addition, serial chains often concentrate trading in a narrower maturity window around the nearby contract month, reducing cross-sectional heterogeneity within each calibration date. We therefore interpret the lower serial RMSE as primarily a horizon-composition effect.

Table 2: Parameter Estimates for Regular and Serial Options (Jan 31, 2019 – Feb 14, 2020)

Parameter	Live Cattle	Feeder Cattle	Corn
Panel A: Regular Options			
Physical (P)			
ω	3.76e-07 [4.21e-07] (9.05e-09)	7.83e-07 [7.50e-07] (6.90e-09)	2.18e-06 [2.18e-06] (3.37e-09)
α	0.0005 [0.0003] (0.0000)	0.0082 [0.0051] (0.0003)	0.0395 [0.0395] (0.0001)
β	0.9905 [0.9898] (0.0002)	0.9661 [0.9706] (0.0005)	0.9421 [0.9414] (0.0002)
γ	0.0113 [0.0123] (0.0002)	0.0370 [0.0356] (0.0002)	0.0287 [0.0286] (0.0002)
Persistence (ϕ)	0.9967 [0.9963] (0.0001)	0.9928 [0.9934] (0.0001)	0.9959 [0.9955] (0.0001)
Risk-Neutral (Q)			
ω^*	5.47e-05 [3.00e-05] (7.00e-06)	6.16e-05 [2.71e-05] (6.68e-06)	5.85e-05 [4.37e-05] (3.31e-06)
α^*	0.1245 [0.0962] (0.0079)	0.1126 [0.0964] (0.0064)	0.0791 [0.0493] (0.0047)
β^*	0.1014 [0.0891] (0.0044)	0.0728 [0.0662] (0.0032)	0.1614 [0.1468] (0.0070)
γ^*	0.2604 [0.2281] (0.0128)	0.3111 [0.3699] (0.0117)	0.1839 [0.2117] (0.0070)
Persistence* (ϕ^*)	0.3561 [0.3790] (0.0100)	0.3410 [0.3604] (0.0105)	0.3324 [0.3208] (0.0070)
Model Fit			
GARCH RMSE	4.27e-04 [3.37e-04] (3.99e-06)	2.74e-04 [2.36e-04] (2.08e-06)	1.28e-03 [1.43e-03] (9.60e-06)
GARCH MAE	1.37e-04 [1.30e-04] (3.39e-07)	1.19e-04 [1.19e-04] (1.44e-07)	3.99e-04 [4.13e-04] (8.56e-07)
FHS RMSE	0.1877 [0.1044] (0.0266)	0.3193 [0.1345] (0.0409)	0.5276 [0.4035] (0.0217)
FHS MAE	0.1586 [0.0811] (0.0256)	0.2848 [0.1127] (0.0398)	0.4047 [0.2961] (0.0178)
Obs.	261	261	261
Panel B: Serial Options			
Risk-Neutral (Q)			
ω^*	6.72e-06 [3.85e-06] (5.84e-07)		1.41e-05 [7.40e-06] (1.22e-06)
α^*	0.0697 [0.0489] (0.0061)		0.1841 [0.1251] (0.0104)
β^*	0.7814 [0.8362] (0.0111)		0.7021 [0.7993] (0.0156)
γ^*	0.0686 [0.0455] (0.0060)		0.0064 [0.0001] (0.0017)
Persistence* (ϕ^*)	0.8854 [0.9095] (0.0058)		0.8894 [0.9181] (0.0071)
Model Fit			
FHS RMSE	0.0486 [0.0434] (0.0026)		0.3655 [0.2297] (0.0202)
FHS MAE	0.0382 [0.0351] (0.0017)		0.2933 [0.1822] (0.0168)
Obs.	261		261

Note: Entries report mean [median] (standard deviation) across daily estimates. Physical parameters are estimated via quasi-maximum likelihood on a rolling 3,500-day window of daily futures log returns. Risk-neutral parameters are calibrated daily by minimizing squared pricing errors between model-implied and market option prices. Persistence is $\phi = \beta + \alpha + \lambda\gamma$, where $\lambda = E[z^2\mathbf{1}(z < 0)]$. GARCH RMSE and MAE measure rolling in-sample conditional variance fit; FHS RMSE and MAE measure option pricing error in dollar terms. Physical (P) parameters for serial options (Panel B) are identical to those reported in Panel A, as the GJR-GARCH is estimated from futures returns only and does not depend on the option cross-section used for risk-neutral calibration. GARCH fit statistics are likewise unchanged.

3.3 Leverage Premium Estimates

Table 3 and Figure 2 report the log leverage premium for regular and serial options. This measure captures the percentage increase in option-implied expected variance attributable to priced asymmetry beyond historical levels. Higher log leverage premia reflect stronger pricing of downside risk. For live cattle regular options, the log leverage premium averages 22% (Table 3), indicating that option-implied expected variance is roughly 22% higher than a counterfactual that preserves historical downside asymmetry. For live cattle serial options, the average is 18%. For feeder cattle, the log leverage premium averages 20%, while corn exhibits a lower average of 11%. The positive corn estimate does not contradict the rightward tilt of grain implied-volatility surfaces documented in Table 1: the leverage premium measures the wedge between option-implied and historical asymmetry, not the direction of the skew. That said, because the GJR specification admits a single asymmetry channel, γ^* is least precisely identified where the surface is flat or right-tilted, and the corn premium should be read with this caveat in mind—consistent with corn's larger pricing errors and the sign divergence between its regular and serial estimates.

Figure 2 plots the daily log leverage premium for each series. Cattle premia run above corn for the full pre-event window (LC regular ≈ 0.22, FC regular ≈ 0.20, ZC regular ≈ 0.11). Corn shows no level shift at August 9 and remains near 0.11 through February 2020. Live cattle regular options rise at the fire and decay to pre-event levels by late December; serial options rise similarly but remain elevated through the end of the sample. This pattern is consistent with a transitory repricing of downside risk following the processing disruption.

Economically, a positive leverage premium means downside variance is priced at a premium in options markets. In practical terms, producers seeking crash protection pay a higher premium for left-tail insurance, while option sellers require greater compensation to bear that downside exposure. Magnitude differences therefore map into hedging-cost differences: contracts with larger leverage premia imply a steeper cost of insuring against adverse price moves, not just higher overall volatility.

These results establish the baseline for our DiD analysis, against which we evaluate whether markets update the pricing of downside-asymmetric volatility risk following a processing disruption.

Table 3: Leverage Premium Decomposition for Regular and Serial Options (Jan 31, 2019 – Feb 14, 2020)

Statistic	Live Cattle	Feeder Cattle	Corn
Panel A: Regular Options			
Expected Realized Variance			
$E^{P}[RV]$	1.60e-04 [1.68e-04] (2.75e-05)	1.23e-04 [1.11e-04] (5.09e-05)	2.80e-04 [2.54e-04] (1.11e-04)
$E^{\tilde{Q}}[RV]$	6.92e-05 [4.82e-05] (1.06e-04)	7.20e-05 [3.84e-05] (1.04e-04)	8.74e-05 [6.29e-05] (7.57e-05)
$E^{Q}[RV]$	8.16e-05 [6.24e-05] (1.07e-04)	8.16e-05 [4.80e-05] (1.04e-04)	9.62e-05 [7.46e-05] (7.91e-05)
Leverage Risk Premium			
VRP Leverage ($E^{Q} - E^{\tilde{Q}}$)	1.24e-05 [7.85e-06] (1.46e-05)	9.54e-06 [6.87e-06] (1.31e-05)	8.89e-06 [7.14e-06] (9.53e-06)
Log Lev. Premium ($\log(E^{Q}/E^{\tilde{Q}})$)	0.22 [0.17] (0.19)	0.20 [0.21] (0.15)	0.11 [0.11] (0.08)
Obs.	261	261	261
Panel B: Serial Options			
Expected Realized Variance			
$E^{P}[RV]$	1.60e-04 [1.69e-04] (2.84e-05)		2.78e-04 [2.51e-04] (1.16e-04)
$E^{\tilde{Q}}[RV]$	8.78e-05 [8.62e-05] (2.82e-05)		1.95e-04 [1.42e-04] (1.28e-04)
$E^{Q}[RV]$	1.04e-04 [9.95e-05] (3.16e-05)		1.96e-04 [1.41e-04] (1.30e-04)
Leverage Risk Premium			
VRP Leverage ($E^{Q} - E^{\tilde{Q}}$)	1.62e-05 [1.39e-05] (1.53e-05)		-1.75e-05 [-1.22e-05] (1.79e-05)
Log Lev. Premium ($\log(E^{Q}/E^{\tilde{Q}})$)	0.18 [0.16] (0.18)		-0.09 [-0.09] (0.07)
Obs.	261		238

Note: Entries report mean [median] (standard deviation) across calibration dates. $E^{P}[RV]$, $E^{\tilde{Q}}[RV]$, and $E^{Q}[RV]$ denote expected realized variance under the physical, counterfactual, and risk-neutral measures, respectively. The log leverage premium is $\log(E^{Q}[RV]/E^{\tilde{Q}}[RV])$. Panel B omits feeder cattle serial options because CME does not list serial contracts for feeder cattle. Serial corn reports 238 observations because 23 calibration dates produce counterfactual persistence $\phi^{\tilde{Q}} = \beta^{*} + \alpha^{*} + \lambda\gamma \geq 1$, violating the stationarity condition required for the closed-form expression; these dates are excluded. All 23 occur in the pre-event period, so the post-event control group is unaffected.

Figure 2: Log Leverage Premium for Regular and Serial Options

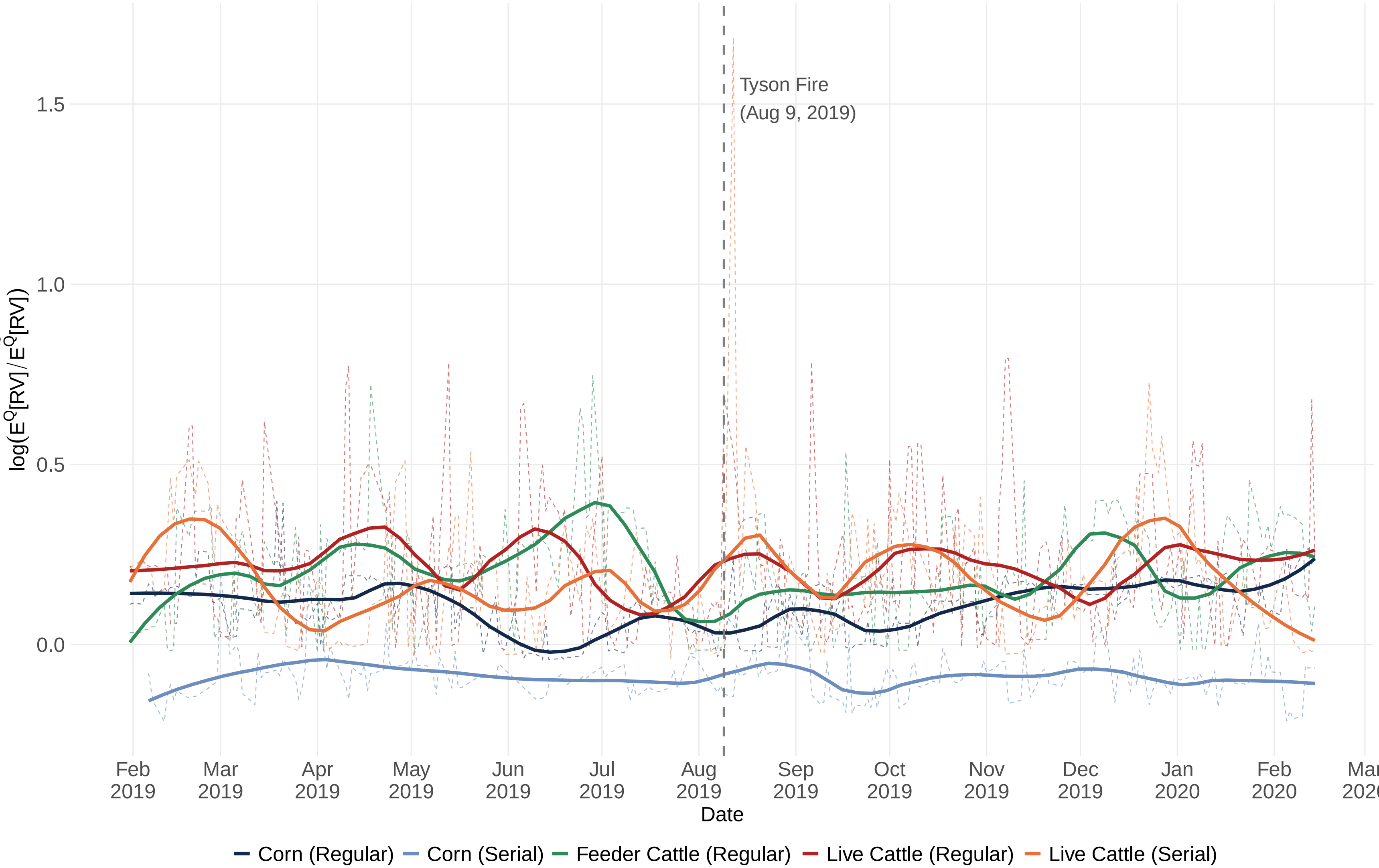

Note: Daily log leverage premium for live cattle (regular and serial), feeder cattle (regular), and corn (regular and serial) options from January 31, 2019 to February 14, 2020. Dashed lines show daily values; solid lines are loess-smoothed trends. The vertical dashed line marks the August 9, 2019 Tyson Holcomb fire.

4 The Tyson Holcomb Fire Natural Experiment

We use the August 9, 2019 fire at Tyson Foods' Holcomb, Kansas beef processing facility as a natural experiment. The shutdown generated a sudden disruption in beef-packing capacity, allowing us to test whether the log leverage premium responds to a realized downside shock. The facility partially resumed operations in November 2019 and returned to near-full capacity by late December 2019 (Dennis, 2020). October live cattle futures declined sharply in the immediate aftermath, consistent with a negative capacity shock.

We estimate a DiD design comparing cattle options (treated commodity)) with corn options (control commodity) before and after the event. Corn is an economically meaningful control because it captures the feed-input side of cattle production and therefore shares broad agricultural and macro conditions with cattle markets, yet it is not directly exposed to the fire's treatment channel, namely a sudden loss of beef-processing capacity. The comparison therefore helps isolate changes in downside-risk pricing that are specific to cattle markets rather than reflecting broader movements in agricultural volatility.

The identifying assumption is that, absent the fire, leverage-premium dynamics in cattle and corn would have followed parallel trends. We report results for three symmetric event windows—72, 107, and 136 business days—corresponding to the shutdown (fire-to-partial-reopening), partial-reopening (fire-to-full-reopening), and the full-reopening periods, respectively. We also implement a bandwidth sensitivity analysis by calculating DiD estimates across all symmetric windows of 25 to 136 business days around the event.

4.1 Specification

Our baseline specification is

$$y_{it} = \alpha + \beta_1 \text{Treated}_i + \beta_2 \text{Post}_t + \beta_3 (\text{Treated}_i \times \text{Post}_t) + \varepsilon_{it}, \tag{8}$$

where y_{it} is the log leverage premium for commodity i on day t, $\text{Treated}_i = 1$ for cattle (live cattle, or feeder cattle in upstream specifications) and 0 for corn, and $\text{Post}_t = 1$ for dates on or after

August 9, 2019. The coefficient of interest is β_3.

To account for potential differences in underlying time trends between treated and control markets, we estimate

$$y_{it} = \alpha + \beta_1 \text{Treated}_i + \beta_2 \text{Post}_t + \beta_3 (\text{Treated}_i \times \text{Post}_t) + \beta_4 \text{Days}_t + \beta_5 (\text{Treated}_i \times \text{Days}_t) + \varepsilon_{it}, \quad (9)$$

where Days_t is calendar time centered at August 9, 2019. We refer to this specification as the +T specification, indicating the baseline model augmented with linear trend controls. The term $\text{Treated}_i \times \text{Days}_t$ lets the treated and control groups follow different linear trends over time. With this control, β_3 captures the immediate level shift at the event date for the treated group relative to the control, after accounting for those underlying trend differences.

Our richest daily specification adds lagged microstructure controls and annual seasonality terms to account for option-market trading conditions and within-year variation in the leverage premium that may influence option prices independently of the processing shock:

$$\begin{aligned} y_{it} = \alpha &+ \beta_1 \text{Treated}_i + \beta_2 \text{Post}_t + \beta_3 (\text{Treated}_i \times \text{Post}_t) + \beta_4 \text{Days}_t + \beta_5 (\text{Treated}_i \times \text{Days}_t) \\ &+ \theta X_{it-1} + \psi_1 \sin\left(\tfrac{2\pi \, \text{DOY}_t}{365}\right) + \psi_2 \cos\left(\tfrac{2\pi \, \text{DOY}_t}{365}\right) + \varepsilon_{it}, \end{aligned} \quad (10)$$

where X_{it-1} includes lagged log volume, volume ratio (current volume divided by 20-day moving average), and open-interest change (log difference). To account for potential seasonality in the dependent variable, we also include annual Fourier terms (sine and cosine functions of day-of-year–DOY) to capture the cattle cycle seasonality. Because trading activity may respond to contemporaneous market conditions, the microstructure variables are lagged one period. These controls account for liquidity-driven movements in implied volatility and changes in market positioning that may affect the leverage premium independently of the processing disruption. We refer to equation (10) as the +T+M specification, where "M" denotes the additional controls: microstructure variables and annual Fourier seasonality terms. We treat this as our preferred specification because it accounts for differential trends, liquidity-related variation in option pricing, and intra-annual seasonality in cattle markets.

We also estimate weekly specifications that include hedging-pressure controls (the +T+HP specification). The Full specification additionally includes the lagged microstructure and Fourier seasonality controls from the +T+M specification. $\mathrm{HP}_{it}^{\mathrm{Long}}$ and $\mathrm{HP}_{it}^{\mathrm{Short}}$ are constructed from CFTC Commitment of Traders data as commercial long and short options positions scaled by open interest (See Appendix Figure B.3 for further details). Because COT data are released weekly, these specifications aggregate the daily panel to one observation per commodity-week. The full specification adds both hedging-pressure and lagged microstructure controls. Hedging-pressure controls are important because the existing literature documents that commercial trading activity can influence option pricing patterns independently of the underlying risk environment (Bessembinder, 1992; De Roon, Nijman, and Veld, 2000, Mckenzie et al 2022). By including these controls, we assess whether the post-fire increase in the leverage premium is robust to observable changes in hedging activity. Because the weekly hedging-pressure specifications substantially reduce the time-series dimension of the panel, we treat them as robustness checks and retain the daily +T+M specification as the primary specification for inference.

All daily specifications report Driscoll-Kraay standard errors (Driscoll and Kraay, 1998), which account for heteroskedasticity, serial correlation, and cross-sectional dependence. With only two cross-sectional units, conventional cluster-robust standard errors are infeasible, and Driscoll-Kraay provides a panel-robust alternative that is well suited to settings with large T and small N. The bandwidth, which controls how many past lags of autocorrelation are incorporated into the Driscoll–Kraay standard errors, is set to $\lfloor 0.75 \times T^{1/3} \rfloor$ following standard practice.

Because the log leverage premium is derived from slowly evolving GARCH parameters and exhibits an AR(1) coefficient of approximately 0.64 in the LC–ZC difference series, asymptotic approximations may not fully capture finite-sample uncertainty even with heteroskedasticity- and autocorrelation-consistent standard errors (Bertrand et al., 2004). We therefore supplement parametric inference with a per-window studentized permutation test calibrated to the symmetric DiD design. For each event window $w \in \{\text{Shutdown}, \text{Partial-Reopening}, \text{Full-Reopening}\}$ and each candidate placebo date d that admits at least w business days of both pre- and post-event data within the sample, we re-estimate the +T+M specification using d as the placebo date and record the studentized statistic $\hat{t}_d = \hat{\beta}_{3,d}/\mathrm{SE}(\hat{\beta}_{3,d})$ on the Treated $\times$ Post interaction. The one-sided permutation p-value for window w is

$$p_w = \frac{1}{K_w} \sum_{d \in \mathcal{D}_w} \mathbf{1}\{\hat{t}_d \geq \hat{t}\}, \tag{11}$$

where $\mathcal{D}_w$ is the set of valid placebo dates, $K_w = |\mathcal{D}_w|$ is the number of admissible placebo dates for event window w, and $\hat{t}$ is the actual studentized statistic at the August 9, 2019 event. All placebo regressions, including the actual regression that supplies the reference statistic, use heteroskedasticity-robust with finite-sample correction standard errors; the permutation procedure absorbs serial dependence nonparametrically, so the correction used in the main DiD specifications is not needed here.

Three design choices deserve note. The symmetric-fit constraint forces every placebo regression to share the actual regression's pre/post structure, so the placebo distribution is constructed under the same pre/post sample geometry as the actual specification. The studentized statistic, rather than raw $\hat{\beta}$, normalizes for variation in estimator precision across placebo dates arising from differing pre/post sample compositions. The one-sided test reflects the directional economic hypothesis that a processing-capacity shock should raise the price of downside protection, not lower it. Because placebo dates near August 9 partially capture the true treatment effect, the absence of an exclusion zone biases p_w upward; the test is therefore conservative. The symmetric-fit constraint leaves only 27 candidate placebo dates for the Full-Reopening window, which is too few for reliable permutation inference.

4.2 Identification and Validity Checks

Identification of the effect of the Holcomb processing disruption on the leverage premium relies on several assumptions and supporting validity checks.

Parallel trends. We test for differential pre-trends by regressing the log leverage premium on Treated, Days, and Treated $\times$ Days using pre-event data. Table 4 reports separate pre-trend regressions using only the pre-event observations corresponding to each symmetric event window. The Shutdown pre-period provides the strongest support for parallel trends, with all coefficients statistically insignificant. Results for the Partial-Reopening and Full-Reopening windows are more mixed, with several coefficients approaching or reaching conventional significance levels; however, these are generally small and do not display a consistent directional pattern. While no design can rule out all concurrent news, the treatment shock itself does not coincide with a scheduled Cattle on Feed release (the nearest releases occur on July 19 and August 23), reducing concern that the estimated discontinuity simply reflects a contemporaneous USDA announcement.

Table 4: Parallel Trends Test: Pre-Event Differential Trends

Pre-period	Panel	Treated × Days	SE	p-value
Shutdown	LC Regular	−0.00082	0.00089	0.364
	LC Serial	−0.00023	0.00082	0.778
	FC Regular	0.00010	0.00143	0.945
Partial-Reopening	LC Regular	−0.00010	0.00048	0.829
	LC Serial	0.00075	0.00041	0.066
	FC Regular	0.00063	0.00068	0.353
Full-Reopening	LC Regular	0.00023	0.00035	0.513
	LC Serial	−0.00074	0.00042	0.084
	FC Regular	0.00105	0.00051	0.041

Note: Pre-event regressions of the log leverage premium on Treated, Days (calendar time centered at August 9, 2019), and Treated × Days, estimated separately for each pre-event window using only observations prior to the Holcomb fire. Pre-trend regressions use only the pre-event portion of each symmetric event window. The corresponding pre-event samples begin on April 30, 2019; March 12, 2019; and January 31, 2019, respectively. Driscoll-Kraay standard errors are reported. The coefficient of interest is $\hat{\beta}$ on Treated × Days; a statistically insignificant estimate supports the parallel trends assumption.

Control validity and limited spillovers. Control validity requires that corn is exposed to general market conditions but not to the treatment channel. To assess potential spillovers, we compare mean corn leverage premia between the pre-event week (August 5–9, 2019) and the first post-event week (August 12–16, 2019) using a Welch unequal-variance$t$-test. We focus on a narrow window around the event because a short-horizon comparison helps isolate the immediate impact of the fire on the control market; over longer horizons, the corn leverage premium may drift for reasons unrelated to the Holcomb shock, making it difficult to distinguish spillovers from unrelated variation in the control market. The corn log leverage premium changes little across the event window ($\Delta = 0.0155$, Welch $p = 0.817$).

Exogeneity of event timing. The Tyson Holcomb fire was an abrupt operational accident, not a scheduled policy intervention, regulatory change, or pre-announced market event. This supports the assumption that treatment timing was unrelated to prior outcome trends. Consistent with this interpretation, cattle futures reacted sharply following the fire, indicating an unanticipated negative processing-capacity shock.

Falsification: feeder cattle placebo test. As a falsification test, we estimate the same DiD specification using feeder cattle as the treated commodity. Because feeder cattle are upstream in the production chain, they should not exhibit a comparable response. Consistent with this prediction, feeder cattle estimates are small, statistically insignificant, and often negative across specifications and event windows (Table 5, Panel C). Permutation p-values for feeder cattle are 0.720 (Shutdown) and 0.607 (Partial-Reopening), supporting the interpretation that the Holcomb shock operated through beef-packing capacity rather than through feed markets or broad agricultural conditions.[3]

4.3 Results

Table 5 reports DiD estimates across three symmetric event windows—Shutdown (72 business days, fire to partial reopening), Partial-Reopening (107 business days, fire to full reopening), and Full-Reopening (136 business days, full balanced sample)—for live cattle regular options, live cattle serial options, and feeder cattle regular options. Permutation-based p-values for the preferred +T+M specification are reported alongside the main estimates where available. Figure 3 displays the bandwidth sensitivity analysis.

[3]The feeder cattle falsification is informative but not fully clean: Table 4 shows a statistically significant positive pre-trend for FC in the Full-Reopening window ($p < 0.05$). Post-event FC estimates are statistically insignificant across all specifications and windows. Because the pre-trend is positive, any resulting bias would tend to generate a positive post-event effect, making the absence of such an effect more, not less, informative. By contrast, the live cattle-corn comparison, which provides the paper's main results, does not exhibit this issue.

Table 5: Difference-in-Differences Estimates: Log Leverage Premium

		(1) Basic	(2) +T	(3) +T+M	(4) +T+HP	(5) Full
Panel A: Live Cattle Regular Options (LC vs. ZC)						
Shutdown	Treated × Post	0.0187	0.1293	0.1374*	0.2690**	0.2902**
		(0.0506)	(0.0881)	(0.0830)	(0.1336)	(0.1215)
	Permutation p-value			[0.053]		
Partial-Reopening	Treated × Post	−0.0203	0.0948	0.0863	0.0771	0.0943
		(0.0411)	(0.0774)	(0.0739)	(0.1040)	(0.1077)
	Permutation p-value			[0.024]		
Full-Reopening	Treated × Post	−0.0171	0.0459	0.0390	0.0040	0.0076
		(0.0348)	(0.0725)	(0.0714)	(0.1086)	(0.1129)
Panel B: Live Cattle Serial Options (LC vs. ZC)						
Shutdown	Treated × Post	0.0925**	0.2223**	0.2329**	0.0438	0.0784
		(0.0450)	(0.1067)	(0.1007)	(0.1089)	(0.1159)
	Permutation p-value			[0.100]		
Partial-Reopening	Treated × Post	0.1283***	0.0954	0.0900	−0.0286	−0.0198
		(0.0401)	(0.0942)	(0.0932)	(0.0866)	(0.0911)
	Permutation p-value			[0.274]		
Full-Reopening	Treated × Post	0.0584	0.2051***	0.1960***	0.1092	0.1022
		(0.0389)	(0.0746)	(0.0732)	(0.0796)	(0.0800)
Panel C: Feeder Cattle Regular Options (FC vs. ZC)						
Shutdown	Treated × Post	−0.0943*	−0.0587	−0.0661	−0.0166	−0.0261
		(0.0481)	(0.1032)	(0.1041)	(0.1426)	(0.1564)
	Permutation p-value			[0.720]		
Partial-Reopening	Treated × Post	−0.0745*	−0.1008	−0.1078	−0.0040	−0.0254
		(0.0395)	(0.0912)	(0.0927)	(0.1134)	(0.1269)
	Permutation p-value			[0.607]		
Full-Reopening	Treated × Post	−0.0467	−0.1343	−0.1379*	−0.0846	−0.1020
		(0.0361)	(0.0827)	(0.0827)	(0.1227)	(0.1292)
Observations (72 / 107 / 136 windows)						
LC Regular			276 / 408 / 520		60 / 90 / 112	
LC Serial			257 / 389 / 498		59 / 89 / 110	
FC Regular			276 / 408 / 520		60 / 90 / 112	
Linear trend			✓	✓	✓	✓
Microstructure + Fourier				✓		✓
Hedging pressure					✓	✓
Data frequency		Daily	Daily	Daily	Weekly	Weekly

Note: The dependent variable is the daily log leverage premium. Each cell reports the $\hat{\beta}_3$ coefficient on Treated × Post from the indicated specification (in columns). Window labels in rows denote symmetric business-day windows around the August 9, 2019 event: 72 spans the fire to partial-reopening (Shutdown), 107 to full reopening (Partial-Reopening), and 136 is the full balanced sample (Full-Reopening). Panels A and B compare live cattle with corn; Panel C compares feeder cattle with corn. Specifications: (1) no controls; (2) linear trend; (3) adds lagged log volume, volume ratio, open-interest change, and annual Fourier seasonality (sin, cos of day-of-year); (4) adds CFTC hedging pressure (weekly frequency); (5) all controls. Driscoll-Kraay standard errors are reported in parentheses. Permutation p-values for the +T+M specification are reported in brackets below the corresponding standard errors. Permutation inference is omitted for the Full-Reopening window because the symmetric-fit constraint leaves only 27 admissible placebo dates. $^{*}p < 0.10$; $^{**}p < 0.05$; $^{***}p < 0.01$, based on Driscoll-Kraay inference.

For live cattle regular options, the strongest evidence of repricing appears in the Shutdown window, which isolates the period of active capacity constraint. In our preferred specification (+T+M), the treated×post coefficient is 0.1374 (Driscoll-Kraay $p = 0.10$; permutation $p = 0.053$), indicating that the log leverage premium increased by approximately 14% for live cattle relative to corn during the disruption. The parsimony check that drops microstructure and seasonality controls (+T) yields a similar coefficient of 0.1293 ($p = 0.141$), suggesting that the magnitude of the estimated effect is broadly stable across the two specifications. Weekly specifications that further include hedging-pressure controls yield larger estimates (+T+HP: 0.2690, $p < 0.05$; Full: 0.2902, $p < 0.05$), though these rely on substantially fewer observations ($N = 60$). The fact that estimates rise once hedging pressure is accounted for is consistent with commercial positioning shifts during the shutdown partially offsetting the underlying repricing in the uncontrolled specifications. Table 6 reports the hedging-pressure coefficients; HP Short is positive and significant for LC Regular in the Shutdown window, indicating that greater commercial short positioning is associated with higher leverage premia. However, the positive DiD estimates remain after controlling for hedging pressure.

Table 6: Hedging Pressure Coefficients (Full Specification)

	Shutdown		Partial-Reopening		Full-Reopening	
	HP Long	HP Short	HP Long	HP Short	HP Long	HP Short
LC Regular	−1.4880	0.8038**	0.0948	0.3845	−0.2379	−0.0479
	(1.2267)	(0.3550)	(0.3941)	(0.3078)	(0.4511)	(0.3338)
LC Serial	−0.2072	−0.6124*	−0.2302	−0.2213	−0.1863	−0.0608
	(0.9400)	(0.3300)	(0.4843)	(0.2852)	(0.5680)	(0.3219)
FC Regular	0.5485	−1.0147	0.5457	−0.3643	0.1939	−0.4407*
	(0.7028)	(1.0901)	(0.3899)	(0.2583)	(0.3597)	(0.2440)

Note: Coefficients on HP Long and HP Short from the Full specification (column 5 of Table 5), which includes linear trend, microstructure controls, annual Fourier seasonality, and CFTC hedging pressure. HP Long and HP Short are commercial long and short hedging pressure from CFTC Commitment of Traders data, constructed as commercial positions scaled by open interest. Weekly data frequency. Driscoll-Kraay standard errors are reported in parentheses. *$p < 0.10$; **$p < 0.05$; ***$p < 0.01$.

As the event window expands to encompass the plant's capacity restoration, the estimated effect attenuates. In the Partial-Reopening window, the +T+M estimate declines to 0.0863 (p

= 0.25; permutation $p = 0.024$); in the Full-Reopening window, it falls to 0.0390 (Driscoll-Kraay $p = 0.59$). This attenuation pattern is consistent with option markets repricing downside risk in response to the shock, rather than fully incorporating it ex ante, with the effect dissipating as processing capacity was restored.

Figure 3: Bandwidth Sensitivity Analysis Differences in Differences

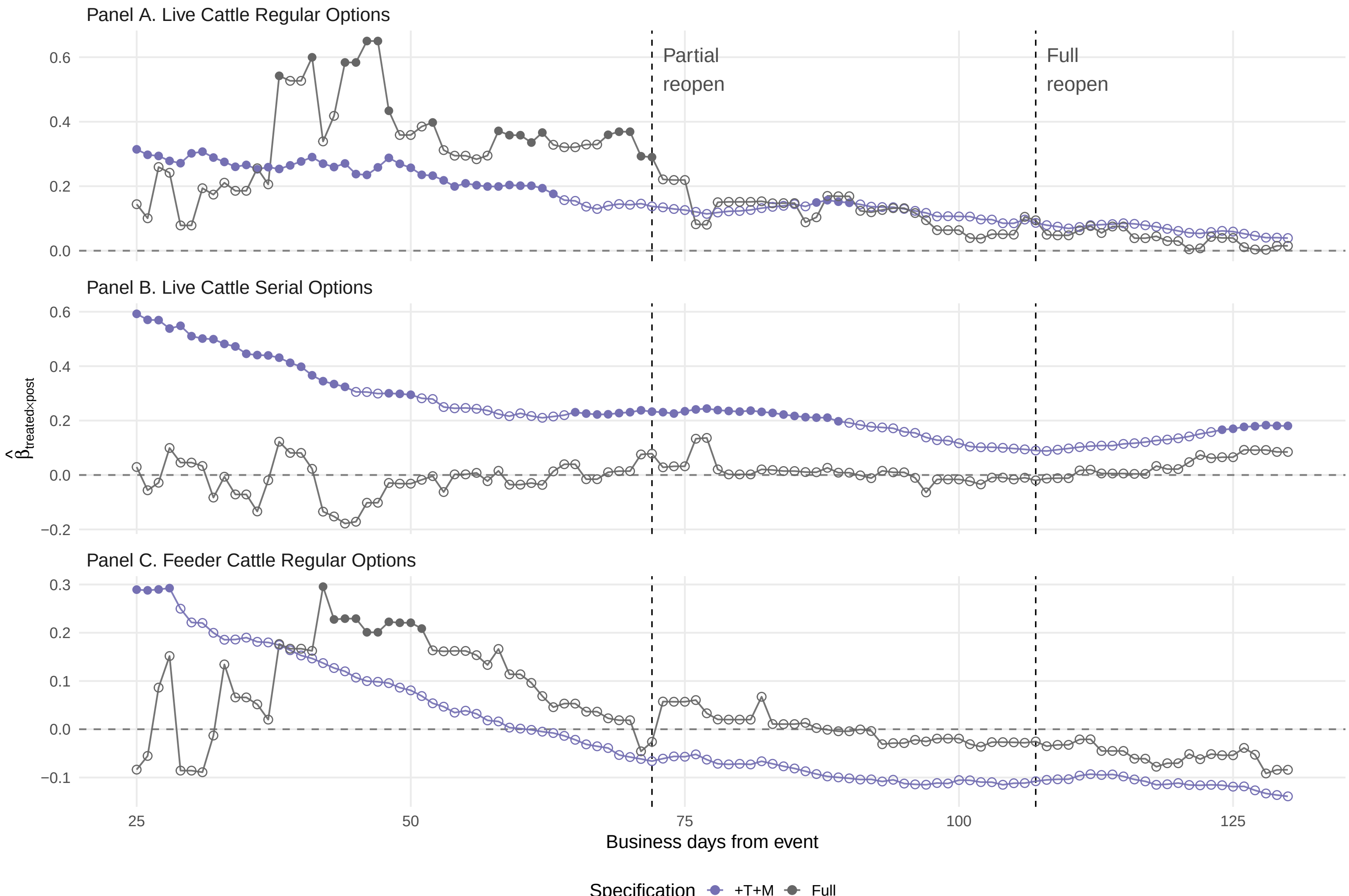

Note: Each panel plots the difference-in-differences coefficient on Treated × Post across symmetric event windows ranging from 25 to 130 business days after the August 9, 2019 Tyson Holcomb fire. Panels A and B compare live cattle regular and serial options to corn; Panel C compares feeder cattle regular options to corn. Series show the preferred +T+M specification (daily) and the Full specification (weekly, with hedging-pressure controls). Filled circles indicate significance at the 5% level; open circles are not significant. Vertical dashed lines mark the partial (72) and full (107) reopening milestones.

Live cattle serial options corroborate the regular-options finding but display a different temporal profile. In the Shutdown window, the preferred +T+M estimate is 0.2329 (Driscoll-Kraay $p = 0.020$; permutation $p = 0.100$), with the parsimony +T specification at 0.2223 ($p = 0.037$) and the basic specification at 0.0925 ($p = 0.039$). Unlike regular options, the serial effect persists at wider windows: the Full-Reopening +T+M estimate is 0.1960 ($p = 0.007$). Despite the higher persistence in the serial-options ($\phi^* = 0.8854$ versus 0.3561 for regular options), the shorter maturities of serial contracts make them more responsive to near-term shifts in downside-risk pricing. Weekly hedging-pressure specifications for serial options are imprecisely estimated ($N \approx 50$–80), with estimates near zero and large standard errors, limiting inference from these specifications.

Feeder cattle options show no evidence of a positive shift in the leverage premium. In the preferred +T+M specification, the treated×post estimate is -0.0661 (Shutdown), -0.1078 (Partial-Reopening), and -0.1379 (Full-Reopening). The non-positive pattern across all windows and specifications confirms that the repricing of downside-asymmetric risk was concentrated in the market most directly exposed to the processing bottleneck.

Figure 3 displays $\hat{\beta}_3$ estimates for all five specifications across symmetric windows of 25 to 136 business days, incremented one day at a time. For live cattle regular options (Panel A), all trend-based specifications produce positive estimates that decline monotonically as the window widens. The +T and +T+M specifications remain positive and are frequently statistically significant at the 5% level for windows up to approximately 55–65 business days, corresponding to the active disruption period. The weekly HP-controlled specifications (+T+HP, Full) produce larger estimated effects at shorter windows before attenuating at wider horizons. Vertical reference lines at the partial and full reopening milestones show that the decline in estimated effects tracks the capacity restoration timeline. For live cattle serial options (Panel B), the +T and +T+M specifications decline monotonically, but remain significant across most windows, consistent with the persistent effect discussed above. For feeder cattle (Panel C), all specifications remain near or below zero across all windows, consistent with the absence of a feeder-cattle treatment effect.

Taken together, these findings indicate that the Holcomb fire was associated with a transitory increase in the market price of downside-asymmetric volatility risk in live cattle options relative to corn. The effect was strongest during the active shutdown, attenuated for regular options as processing capacity was restored, and persisted in serial options. Feeder cattle showed no comparable response. The increase in the leverage premium also remained positive after controlling for observable commercial hedging activity, suggesting that the repricing reflected more than shifts in hedging demand alone. These patterns are consistent with option markets revising the pricing of downside risk following a realized disruption, with the effect attenuating as underlying supply conditions normalized.

4.4 Economic Magnitude

Section 4.3 shows that, in the preferred Shutdown specification (+T+M), the fire increased the live-cattle log leverage premium by about 0.14 log points relative to corn. To gauge the economic size of that repricing, we map the estimate into the implied cost of a representative short-dated OTM put option using a local Black (1976) approximation. The estimated dollar hedging costs are approximate because they are inferred from changes in the leverage premium rather than measured directly from option prices.

The calculation proceeds in three steps. First, we map the estimated change in the log leverage premium into an increase in risk-neutral expected variance. Second, using a local Black (1976) approximation, we convert that variance increment into an implied-volatility increase. Third, we apply Black vega to translate the implied-volatility increase into a dollar increase in put-option premia.

The DiD coefficient implies that the ratio of risk-neutral to counterfactual expected variance increased by a factor of $e^{0.14} \approx 1.15$ for live cattle relative to corn during the active disruption. This corresponds to approximately a 15% increase in the leverage-premium ratio. Define the baseline leverage-premium ratio as $R_0 \equiv E^{\mathbb{Q}}[RV]_0 / E^{\tilde{\mathbb{Q}}}[RV]_0$ so that the baseline risk-neutral variance is $E^{\mathbb{Q}}[RV]_0 = E^{\tilde{\mathbb{Q}}}[RV]_0 \times R_0$. Multiplying the estimated percentage increase by this baseline risk-neutral variance yields the implied increase in expected variance. Using baseline values from Table 3, $E^{\tilde{\mathbb{Q}}}[RV]_0 \approx 6.92 \times 10^{-5}$ and a sample-average log leverage premium of approximately 0.22 (implying $R_0 = e^{0.22} \approx 1.246$), the fire-induced increment in expected daily variance is

$$\Delta E^{\mathbb{Q}}[RV] \;=\; E^{\tilde{\mathbb{Q}}}[RV]_0 \times R_0 \times \left(e^{0.14} - 1\right) \;\approx\; 6.92 \times 10^{-5} \times 1.246 \times 0.150 \;\approx\; 1.29 \times 10^{-5}, \quad (12)$$

or approximately 0.0033 in annualized variance terms ($1.29 \times 10^{-5} \times 252$).[4]

For short-dated OTM options not too far from the money, Black (1976) implied variance provides a useful local approximation to risk-neutral expected realized variance.[5] To convert this variance increment into a volatility change, we linearize $\sigma = \sqrt{v}$ around the pre-fire annualized implied variance for OTM live cattle puts in the $[0.85, 1.00)$ moneyness range ($\bar{\sigma} \approx 0.184$ from Table 1, so $\bar{\sigma}^2 \approx 0.034$). Writing Δv for the annualized variance increment, a first-order Taylor expansion of $\sqrt{v}$ around $\bar{\sigma}^2$ gives

$$\Delta\sigma \approx \frac{\Delta v}{2\bar{\sigma}} = \frac{0.0033}{2 \times 0.184} \approx 0.009, \tag{11}$$

so the repricing implies roughly 0.9 percentage points of additional implied volatility.[6]

The final step translates the implied-volatility increase into option prices using Black (1976) vega, which measures the sensitivity of an option's price to a one-percentage-point change in implied volatility. For representative OTM puts with futures price $F = 110$ \$/cwt and $\tau = 45/252$ trading days, Black (1976) vega ranges from approximately \$58 per contract per percentage point at $K/F = 0.95$ to roughly \$68 at $K/F = 0.97$.[7] Applied to a 0.9 percentage-point volatility increase, this implies an incremental put cost on the order of \$50–\$60 per contract. Since one live cattle contract covers 40,000 lbs, or roughly 31 head at a market weight of approximately 1,300 lbs, the implied increase in hedge cost is roughly \$1.60–\$1.90 per head.

These magnitudes are economically meaningful in context. The Sterling Beef Profit Tracker reported feedyard margins near breakeven in early June 2019, and by mid-October average closeouts showed a \$10 per head loss that was itself a \$154 per head improvement from the prior month, implying losses exceeding \$160 per head at the peak of the shutdown.[8] An additional hedging cost

[4] See Appendix A for details of the derivation.

[5] This relationship holds exactly for variance swaps and approximately for short-dated options near the money; the approximation weakens for deep OTM strikes and longer maturities.

[6] The linearization is accurate when Δv is small relative to $\bar{\sigma}^2$. Here $\Delta v/\bar{\sigma}^2 \approx 0.0033/0.034 \approx 0.10$, so the first-order term dominates.

[7] Under Black (1976), $d_1 = [\ln(F/K) + \frac{1}{2}\sigma^2\tau]/(\sigma\sqrt{\tau})$, giving vega $= Fe^{-r\tau}\sqrt{\tau}\phi(d_1)$ in ¢/cwt per unit σ, scaled by 400 cwt per contract. The range reflects variation across strikes in the $[0.85, 1.00)$ moneyness bin reported in Table 1.

[8] The Sterling Beef Profit Tracker, calculated by Sterling Marketing (Vale, Oregon), provides weekly benchmark estimates of average cash cattle feeding margins. For 2019, Sterling projected average feedyard profits of \$33 per head ("Profit Tracker: Feeding Margins Near

of a few dollars per head was therefore nontrivial, particularly because it arose precisely when the processing disruption made downside protection most valuable. This monetization is anchored to the preferred live-cattle regular Shutdown estimate, the window in which the repricing effect is strongest.

5 Conclusion

Previous literature documents pronounced downside asymmetry in livestock option markets, reflected in the leftward implied-volatility smirk observed in live and feeder cattle options. We build on this insight and develop a framework to estimate the leverage premium, defined as the component of the variance risk premium attributable to option-implied downside asymmetry beyond historical levels.

Within the filtered historical simulation (FHS) framework of Barone-Adesi et al. (2008), we construct a counterfactual measure that separates historical downside asymmetry from option-implied variance expectations. This decomposition provides a daily measure of the compensation embedded in option prices for downside risk and can be applied to other commodity markets and disruption events.

While pronounced downside skewness in livestock options is well documented, less is known about how those premiums evolve following realized adverse shocks, and whether the smirk primarily reflects downside-risk pricing or commercial hedging pressure. We use the August 2019 Tyson Holcomb fire and a difference-in-differences design to test whether option markets revise the leverage premium following a major supply-chain disruption. Using corn as the control, we find that the leverage premium increased for live cattle during the disruption and attenuated as processing capacity was restored. This finding is supported by both parametric (Driscoll-Kraay) and distribution-free (permutation) inference, and is robust across specification choices.

The repricing was concentrated in live cattle options, the contract most directly exposed to the processing bottleneck created by the fire, while feeder cattle options showed no comparable response. The repricing also remained positive after controlling for observable commercial hedging

Breakeven," *Drovers*, October 22, 2019). Accessed via reprint at `https://cattlemensharrison.com/profit-tracker-feeding-margins-near-breakeven/`

activity, suggesting that the increase in the leverage premium reflected more than shifts in hedging pressure alone. Translated into hedging costs, the live cattle repricing implies roughly \$1.60–1.90 per head in additional put-option cost during the shutdown, an economically meaningful increment given that feedyard margins were near breakeven.

The estimated magnitude may not generalize to all future disruptions. Nevertheless, the live-cattle evidence supports the conjecture that when a shock is large enough to materially worsen downstream marketing conditions, the leverage premium may increase as option markets demand greater compensation for bearing downside risk. This suggests the magnitude of such disruptions was not fully reflected in option-implied downside-risk compensation ex ante. For hedgers, the implication is straightforward: following severe supply-chain disruptions, downside protection may become more expensive precisely when it is most valuable, and that effect persists until the underlying supply conditions normalize, as the attenuation of estimates across capacity restoration milestones confirms.

References

Acharya, V. V., Lochstoer, L. A., & Ramadorai, T. (2013). Limits to arbitrage and hedging: Evidence from Commodity Markets. *Journal of Financial Economics*, 109(2), 441–465. https://doi.org/10.1016/j.jfineco.2013.03.003

Angrist, J. D., & Pischke, J.-S. (2009). Mostly harmless econometrics: An empiricist's companion. Princeton University Press.

Barone-Adesi, G., Engle, R. F., & Mancini, L. (2008). A GARCH option pricing model with filtered historical simulation. *Review of Financial Studies*, 21(3), 1223–1258. https://doi.org/10.1093/rfs/hhn031

Bessembinder, H. (1992). Systematic risk, hedging pressure, and risk premiums in futures markets. *Review of Financial Studies*, 5(4), 637–667. https://doi.org/10.1093/rfs/5.4.637

Bertrand, M., Duflo, E., & Mullainathan, S. (2004). How much should we trust differences-in-differences estimates? *The Quarterly Journal of Economics*, 119(1), 249–275. https://doi.org/10.1162/003355304772839588

Bessembinder, H., Coughenour, J. F., Seguin, P. J., & Smoller, M. M. (1995). Mean reversion in equilibrium asset prices: Evidence from the futures term structure. *The Journal of Finance*, 50(1), 361–375. https://doi.org/10.2307/2329250

Black, F. (1976). The pricing of commodity contracts. *Journal of Financial Economics*, 3(1–2), 167– 179. https://doi.org/10.1016/0304-405X(76)90024-6

Bollerslev, T., Tauchen, G., & Zhou, H. (2009). Expected stock returns and variance risk premia. *Review of Financial Studies*, 22(11), 4463–4492. https://doi.org/10.1093/rfs/hhp008

Bozic, M., & Fortenbery, T. R. (2010). Theory of storage and option pricing: Analyzing determinants of implied skewness and implied kurtosis. Proceedings of the NCCC-134 Conference on Applied Commodity Price Analysis, Forecasting, and Market Risk Management. 10.22004/ag.econ.285313

Bozic, M., Newton, J., Cameron, S., & Gould, B. W. (2012). Parametric bootstrap tests for futures price and implied volatility biases with application to rating livestock margin insurance for dairy cattle. University of Minnesota, St. Paul. http://purl.umn.edu/135077

Bozic, M., Newton, J., Thraen, C. S., & Gould, B. W. (2012). Do Volatility Smiles Matter for Pricing Asian Basket Options? The Case of Livestock Gross Margin Insurance for Dairy Cattle. University of Wisconsin Madison. http://dairy.wisc.edu/pubpod/pubs/wp12-02.pdf

Carr, P., & Wu, L. (2009). Variance risk premiums. *Review of Financial Studies*, 22(3), 1311–1341. https://doi.org/10.1093/rfs/hhn038

Carriquiry, M., Elobeid, A., Hayes, D., & Zhang, W. (2019). Impact of African swine fever on U.S. and world commodity markets. Agricultural Policy Review, Fall 2019. Center for Agricultural and Rural Development, Iowa State University. `https://www.card.iastate.edu/ag_policy_review/article/?a=101`

Chavas, J. P., Li, J., & Wang, L. (2024). Option pricing revisited: The role of price volatility and dynamics. *Journal of Commodity Markets*, 33, 100381. https://doi.org/10.1016/j.jcomm.2023.100381

CME Group. (2014, January). An introduction to cattle feeding spreads. CME Group. `https://www.cmegroup.com/trading/agricultural/files/AC-378_CattleFeedingWhitePaper_r2.pdf`

Dennis, E. (2020, September 11). A Historical Perspective on the Holcomb Fire: Differences and Similarities to the COVID-19 Situation and Other Significant Market Events, University of Nebraska–Lincoln. Retrieved from: https://cap.unl.edu/news/historical-perspective-holcomb-fire-differences-and-similarities-covid-19-situation-and-other/

De Roon, F. A., Nijman, T. E., & Veld, C. (2000). Hedging pressure effects in futures markets. *The Journal of Finance*, 55(3), 1437–1456. https://doi.org/10.1111/0022-1082.00253

Duan, J. C., & Simonato, J.G. (1998). Empirical martingale simulation for asset prices. *Management Science*, 44(9), 1218–1233. https://doi.org/10.1287/mnsc.44.9.1218

Dumas, B., Fleming, J., & Whaley, R. E. (1998). Implied volatility functions: Empirical tests. *Journal of Finance*, 53(6), 2059–2106. https://www.jstor.org/stable/117461

Engle, R. F., & Ng, V. K. (1993). Measuring and testing the impact of news on volatility. *The Journal of Finance*, 48(5), 1749–1778. https://doi.org/10.1111/j.1540-6261.1993.tb05127.x

Etula, E. (2013). Broker-dealer risk appetite and commodity returns. *Journal of Financial Econometrics*, 11(3), 486–521. https://doi.org/10.1093/jjfinec/nbs024

Goodwin, B. K., Harri, A., Rejesus, R. M., & Coble, K. H. (2017). Measuring price risk in rating revenue coverage: BS or no BS? *American Journal of Agricultural Economics*, 100(2), 456–478. https://doi.org/10.1093/ajae/aax083

Glosten, L. R., Jagannathan, R., & Runkle, D. E. (1993). On the relation between the expected value and the volatility of the nominal excess return on stocks. *The Journal of Finance*, 48(5), 1779– 1801. https://doi.org/10.1111/j.1540-6261.1993.tb05128.x

McKenzie, A. M., Thomsen, M. R., & Adjemian, M. K. (2022). Characterizing implied volatility functions from agricultural options markets. *American Journal of Agricultural Economics*, 104(5), 1605–1624. https://doi.org/10.1111/ajae.12288

Nelder, J. A., & R. Mead. (1965). A simplex method for function minimization. *The Computer Journal*, 7(4), 308-313.

Hart, C. E., Lence, S. H., Hayes, D. J., & Jin, N. (2016). Price mean reversion, seasonality, and options markets. *American Journal of Agricultural Economics*, 98(3), 707–725. https://doi.org/10.1093/ajae/aav045

Hu, Z., Mallory, M., Serra, T., & Garcia, P. (2020). Measuring price discovery between nearby and deferred contracts in storable and nonstorable commodity futures markets. *Agricultural Economics*, 51(6), 825–840. https://doi.org/10.1111/agec.12594

Peel, D. S. (2003). Beef cattle growing and backgrounding programs. *Veterinary Clinics of North America: Food Animal Practice*, 19(2), 365–385. https://doi.org/10.1016/s0749-0720(03)00032-x

Sørensen, C. (2002). Modeling seasonality in agricultural commodity futures. *Journal of Futures Markets*, 22(5), 393–426. https://doi.org/10.1002/fut.10017

Thomsen, M. R., & McKenzie, A. M. (2010). Measuring and explaining skewness in pricing distributions implied from livestock options. Paper presented at the NCCC-134 Conference on Applied Commodity Price Analysis, Forecasting, and Market Risk Management, St. Louis, MO, April 19–20. 10.22004/ag.econ.285330

Thomsen, M., McKenzie, A. M., & Power, G. J. (2013). Was there a peso problem in cattle options? Evidence from the 2003 bovine spongiform encephalopathy announcement. *Agricultural Finance Review*, 73(3), 526–538. https://doi.org/10.1108/AFR-09-2012-0048

Trujillo-Barrera, A., Garcia, P., & Mallory, M. L. (2017). Short-term price density forecasts in the Lean Hog Futures Market. *European Review of Agricultural Economics*, 45(1), 121–142. https://doi.org/10.1093/erae/jbx026

Turvey, C. G., & Komar, S. (2007). Martingale restrictions and the implied market price of Risk. *Canadian Journal of Agricultural Economics/Revue Canadienne d'agroeconomie*, 55(1), 138– 158. https://doi.org/10.1111/j.1744-7976.2007.00084_2.x

U.S. Department of Agriculture, Agricultural Marketing Service. (2020, July 22). Boxed beef & fed cattle price spread investigation report. https://www.ams.usda.gov/sites/default/files/media/CattleandBeefPriceMarginReport.pdf

Zhu, C., Byrd, R. H., Lu, P., & Nocedal, J. (1997). Algorithm 778: L-BFGS-B. *ACM Transactions on Mathematical Software*, 23(4), 550–560. https://doi.org/10.1145/279232.279236

A Appendix Methodological Details

This appendix provides derivations and implementation details for the filtered historical simulation (FHS) framework and leverage premium construction summarized in Section 2. Our empirical strategy exploits the distinction between how volatility has historically behaved and how markets price it today: physical (P) dynamics estimated from past futures returns describe historical volatility evolution, while risk-neutral (Q) dynamics inferred from option prices describe the state-price–weighted distribution used for valuation. The wedge between Q and P is economically meaningful because it reflects compensation embedded in option prices for risks that are not fully spanned by trading in the underlying.

A.1 Option Pricing Under Risk-Neutral Expectations

Following Barone-Adesi, Engle, and Mancini (2008), the time-t price ψ_t of an option with maturity payoff ψ_T is the discounted risk-neutral expectation:

$$\psi_t = E^Q\big[e^{-r\tau}\psi_T \mid \mathcal{F}_t\big] = e^{-r\tau}\int_0^\infty \psi_T(F_T)\, q_{t,T}(F_T)\, dF_T, \tag{1}$$

where F_T denotes the terminal futures price, $\tau = T - t$ is time to maturity, r is the risk-free rate, and $q_{t,T}(\cdot)$ is the risk-neutral density. For European options, the payoff is $\psi_T(F_T) = \max(F_T - K, 0)$ for a call and $\psi_T(F_T) = \max(K - F_T, 0)$ for a put. Because the paper's empirical objects are constructed from P-estimated dynamics and Q-calibrated dynamics, we work directly with the risk-neutral expectation representation.

For futures options, the martingale restriction has a simple interpretation: the time-t futures price for delivery at T equals the Q-expectation of the terminal futures price F_T. Let $F_{t,T}$ denote the time-t futures price for delivery at T. Then $E^Q[F_T \mid \mathcal{F}_t] = F_{t,T}$. We enforce this restriction numerically via empirical martingale simulation.

A.2 Return and Variance Dynamics Under P and Q

The physical measure P captures historical return behavior, while the risk-neutral measure Q reflects pricing dynamics implied by market option prices. Because volatility risk is not perfectly spanned, multiple risk-neutral measures are consistent with arbitrage-free pricing, enabling the empirical modeling strategy of Barone-Adesi et al. (2008).

We model log return dynamics under P using the GJR-GARCH(1,1) specification of Glosten, Jagannathan, and Runkle (1993), which allows conditional variance to respond asymmetrically to negative return innovations:

$$\log\left(\frac{F_t}{F_{t-1}}\right) = \mu + \varepsilon_t, \tag{2}$$

$$\sigma_{t+1}^2 = \omega + \beta\sigma_t^2 + \alpha\varepsilon_t^2 + \gamma I_t \varepsilon_t^2, \tag{3}$$

where $\varepsilon_t = \sigma_t z_t$, $z_t \sim f(0,1)$ are i.i.d. standardized innovations drawn from the empirical distribution of historical residuals, and $I_t = \mathbf{1}(\varepsilon_t < 0)$ indicates negative return innovations. Values of $\gamma > 0$ indicate that negative shocks have a greater impact on conditional variance than positive shocks of the same magnitude.

Under the risk-neutral measure Q, we employ the same GJR-GARCH functional form but allow the parameters to differ from those under P. This reflects that pricing dynamics need not coincide with the historical data-generating process in incomplete markets:

$$\sigma_i^2 = \omega^* + \beta^*\sigma_{i-1}^2 + \alpha^*\varepsilon_{i-1}^2 + \gamma^* I_{i-1}\varepsilon_{i-1}^2, \tag{4}$$

where index t refers to historical time steps for parameter estimation under P, while i denotes simulated steps used in Q-pricing over $i = t+1, \ldots, t+\tau$. The innovations $\varepsilon_i = \sigma_i z_i$ maintain the same empirical distribution as under P, preserving the innovation structure while allowing for parameter flexibility.

Parameter interpretation. The divergence between the physical parameters $\theta = \{\mu, \omega, \beta, \alpha, \gamma\}$ and their risk-neutral counterparts $\theta^* = \{\omega^*, \beta^*, \alpha^*, \gamma^*\}$ reflects the market price of risk embedded in option valuations. While θ is estimated from historical return data and captures historical volatility dynamics, θ^* is extracted from current option prices and incorporates forward-looking risk adjustments.

The α parameter governs how recent return shocks influence next period's conditional variance—the short-run responsiveness of volatility to new information. When $\alpha^* > \alpha$, markets price in stronger immediate volatility responses than historically observed. Similarly, $\beta^* > \beta$ indicates expectations of greater volatility persistence. When $\gamma^* > \gamma$, market participants price in heightened sensitivity to downside risk, placing greater weight on adverse return scenarios when valuing options. Consequently, γ^* embeds a premium for protection against negative shocks, making it a forward-looking indicator of perceived left-tail risk. This difference is the basis of the leverage premium studied in the main text.

Define $\lambda \equiv E[z^2 \mathbf{1}(z < 0)]$, computed from the empirical innovation distribution (equal to 1/2 under symmetry). Persistence captures how long a volatility shock influences future variance and is summarized in GJR-GARCH models by the term $\beta + \alpha + \lambda\gamma$ under P and $\beta^* + \alpha^* + \lambda\gamma^*$ under Q. Differences between physical and risk-neutral persistence reflect how market expectations of volatility dynamics diverge from historical patterns.

A.3 Filtered Historical Simulation Algorithm

We estimate θ by quasi-maximum likelihood (Gaussian QML), which is standard in GARCH applications and remains valid under mild conditions even when innovations are non-normal. For each date, we employ a rolling 3,500-day window of past daily futures log returns to estimate the model under P. We derive the risk-neutral parameter set θ^* through calibration to minimize squared pricing errors between model-implied and market option prices.

We do not impose a closed-form expression for the risk-neutral drift. Instead, we enforce the no-arbitrage martingale restriction numerically using empirical martingale simulation

(Duan and Simonato, 1998). The calibration relies on the FHS approach from Barone-Adesi et al. (2008). In the option-pricing step, $F_{t,T}$ denotes the observed futures price with maturity T corresponding to the option being priced; F_t denotes the nearby futures used in the physical return estimation. For a given day t:

Step 1: Initialization. Use θ as starting values for the optimizer when calibrating θ^*.

Step 2: Path simulation. Let $T = t + \tau$ denote the option maturity date in trading days. For each candidate parameter set θ^* evaluated in the optimization process, simulate $L = 20{,}000$ price paths from t to T. For each path l:

- Draw innovations $z_{[1]}, z_{[2]}, \ldots, z_{[\tau]}$ randomly with replacement from the empirical distribution of standardized daily innovations from the physical GARCH estimation.
- Initialize with F_t and σ_{t+1}^2, where σ_{t+1}^2 is taken from the physical model and serves as the initial variance state for the Q-measure simulation.
- For each simulated step $i = t + 1, \ldots, T$:
  - Compute innovation: $\varepsilon_i = \sigma_i z_{[i-t]}$.
  - Update price: $F_i = F_{i-1} \exp\left(-\frac{1}{2}\sigma_i^2 + \varepsilon_i\right)$.
  - If $i < T$, update variance for the next step:

$$\sigma_{i+1}^2 = \omega^* + \beta^* \sigma_i^2 + \alpha^* \varepsilon_i^2 + \gamma^* I_i \varepsilon_i^2, \tag{5}$$

    where $I_i = \mathbf{1}(\varepsilon_i < 0)$.
- Store the terminal price $F_T^{(l)}$.

We simulate without imposing an explicit drift term; EMS rescales terminal prices to satisfy the martingale restriction.

Step 3: Empirical martingale simulation. Following Duan and Simonato (1998), correct terminal prices to ensure expected values equal the futures price:

- Compute the average simulated terminal price: $\bar{F}_T = \frac{1}{L}\sum_{l=1}^{L} F_T^{(l)}$.
- Let $F_{t,T}$ denote the observed futures price at date t for maturity T.
- Compute the correction factor: $c = F_{t,T}/\bar{F}_T$.
- Adjust all terminal prices: $\tilde{F}_T^{(l)} = c \cdot F_T^{(l)}$ for $l = 1, \ldots, L$.

This ensures that $\frac{1}{L}\sum_{l=1}^{L} \tilde{F}_T^{(l)} = F_{t,T}$, so simulated terminal values are consistent with the futures curve (martingale condition for the futures price under Q).

Step 4: Option pricing. Using corrected terminal prices, compute model prices for all options $j = 1, \ldots, N_t$:

- For calls: $C_j = e^{-r\tau} \cdot \frac{1}{L}\sum_{l=1}^{L} \max\Big(\tilde{F}_T^{(l)} - K_j, 0\Big)$.
- For puts: $P_j = e^{-r\tau} \cdot \frac{1}{L}\sum_{l=1}^{L} \max\Big(K_j - \tilde{F}_T^{(l)}, 0\Big)$.

Step 5: Optimization. Find the risk-neutral parameters that minimize the mean squared pricing error:

$$\theta^* = \arg\min_{\theta^*} \sum_{j=1}^{N_t} [\text{Model Price}_j(\theta^*) - \text{Market Price}_j]^2 \tag{6}$$

subject to the constraints: $\omega^* > 0$ (positive unconditional variance); $\alpha^* \geq 0$, $\beta^* \geq 0$, $\gamma^* \geq 0$ (non-negative coefficients); and $\beta^* + \alpha^* + \lambda\gamma^* < 1$ (stationarity condition).

We employ the Nelder-Mead simplex algorithm (Nelder and Mead, 1965), which does not require gradient computations and is robust to the Monte Carlo noise inherent in the objective function. We use 20,000 simulation paths following Barone-Adesi et al. (2008) with convergence tolerance of 0.0001 and maximum iterations of 800. In cases where Nelder-Mead fails to converge, we employ L-BFGS-B (Zhu et al., 1997) as a fallback optimization method. Calibration is performed using OTM options with greater than 14 business days to expiration as in Barone-Adesi et al. (2008).

A.4 Leverage Premium: Closed-Form Derivation

The divergence between physical and risk-neutral parameters has implications for the pricing of variance risk. Following Carr and Wu (2009), we define the variance risk premium (VRP) as the difference between expected realized variance under the risk-neutral and physical measures. Letting $RV_{t,T} \equiv \frac{1}{\tau}\sum_{i=t+1}^{T}\sigma_i^2$ denote realized variance over the horizon:

$$VRP_{t,T} = E^Q[RV_{t,T} \mid \mathcal{F}_t] - E^P[RV_{t,T} \mid \mathcal{F}_t]. \tag{7}$$

Positive values indicate that option-implied expected variance exceeds historical expected variance.

To isolate the contribution of leverage effect pricing, we construct a counterfactual measure $\tilde{Q}$ with parameters $(\omega^*, \beta^*, \alpha^*, \gamma)$—adopting option-implied base dynamics while retaining the historical leverage response. This counterfactual represents a hypothetical market that has repriced base volatility dynamics using information from options, but has not adjusted its view on asymmetric downside risk beyond historical patterns. The total VRP decomposes as:

$$VRP_{t,T} = \underbrace{E^Q[RV_{t,T} \mid \mathcal{F}_t] - E^{\tilde{Q}}[RV_{t,T} \mid \mathcal{F}_t]}_{VRP_{t,T}^{leverage}} + \underbrace{E^{\tilde{Q}}[RV_{t,T} \mid \mathcal{F}_t] - E^P[RV_{t,T} \mid \mathcal{F}_t]}_{VRP_{t,T}^{base}}. \tag{8}$$

The base component reflects the repricing of the variance level and persistence when moving from historical dynamics to option-implied dynamics. The leverage component isolates the marginal contribution of option-implied asymmetric shock pricing. This leverage component is the empirical object analyzed in the DiD specifications in Section 4.

Step 1: One-step-ahead conditional expectation. The variance recursion implies that σ_{t+1}^2 is $\mathcal{F}_t$-measurable, computed from data through time t. For any measure $J \in \{P, \tilde{Q}, Q\}$ with parameters $(\omega^J, \beta^J, \alpha^J, \gamma^J)$, the variance recursion gives:

$$\sigma_{t+2}^2 = \omega^J + \beta^J \sigma_{t+1}^2 + \alpha^J \varepsilon_{t+1}^2 + \gamma^J I_{t+1} \varepsilon_{t+1}^2. \tag{9}$$

Taking expectations conditional on $\mathcal{F}_t$:

$$E^J[\sigma_{t+2}^2 \mid \mathcal{F}_t] = \omega^J + \beta^J \sigma_{t+1}^2 + \alpha^J E^J[\varepsilon_{t+1}^2 \mid \mathcal{F}_t] + \gamma^J E^J[I_{t+1} \varepsilon_{t+1}^2 \mid \mathcal{F}_t]. \tag{10}$$

Since $\varepsilon_{t+1} = \sigma_{t+1} z_{t+1}$ with z_{t+1} independent of $\mathcal{F}_t$ and $E[z_t^2] = 1$:

$$E^J[\varepsilon_{t+1}^2 \mid \mathcal{F}_t] = \sigma_{t+1}^2 E[z_{t+1}^2] = \sigma_{t+1}^2. \tag{11}$$

For the leverage term:

$$E^J[I_{t+1} \varepsilon_{t+1}^2 \mid \mathcal{F}_t] = \sigma_{t+1}^2 E[z_{t+1}^2 \cdot \mathbf{1}(z_{t+1} < 0)] \equiv \lambda \sigma_{t+1}^2, \tag{12}$$

where $\lambda = \frac{1}{n} \sum_{s=1}^{n} z_s^2 \cdot \mathbf{1}(z_s < 0)$ represents the expected contribution of negative shocks to variance, computed from the empirical innovation distribution. Note that we have the same empirical innovation distribution under P, $\tilde{Q}$, and Q; hence λ is identical across measures. Substituting:

$$E^J[\sigma_{t+2}^2 \mid \mathcal{F}_t] = \omega^J + \phi^J \sigma_{t+1}^2, \tag{13}$$

where $\phi^J = \beta^J + \alpha^J + \lambda \gamma^J$ is the effective persistence under measure J. This establishes that conditional expected variance follows a first-order autoregressive process.

Step 2: Iteration to k-steps ahead. Define $m_k \equiv E^J[\sigma^2_{t+1+k} \mid \mathcal{F}_t]$, so $m_0 = \sigma^2_{t+1}$. From Step 1 applied at horizon $t+1+k$:

$$E^J[\sigma^2_{t+2+k} \mid \mathcal{F}_t] = \omega^J + \phi^J \sigma^2_{t+1+k}. \tag{14}$$

Taking $E^J[\cdot \mid \mathcal{F}_t]$ on both sides and using the tower property yields:

$$m_{k+1} = \omega^J + \phi^J m_k. \tag{15}$$

This is a first-order linear difference equation with solution:

$$m_k = \bar{\sigma}^{2,J} + (\phi^J)^k(\sigma^2_{t+1} - \bar{\sigma}^{2,J}), \tag{16}$$

Proof. The fixed point of the recursion satisfies

$$m = \omega^J + \phi^J m,$$

so

$$m = \frac{\omega^J}{1 - \phi^J}.$$

Define this fixed point as

$$\bar{\sigma}^{2,J} \equiv \frac{\omega^J}{1 - \phi^J}.$$

Let

$$d_k \equiv m_k - \bar{\sigma}^{2,J}.$$

Then

$$\begin{aligned} d_{k+1} &= m_{k+1} - \bar{\sigma}^{2,J} \\ &= (\omega^J + \phi^J m_k) - \bar{\sigma}^{2,J} \\ &= (\omega^J + \phi^J m_k) - (\omega^J + \phi^J \bar{\sigma}^{2,J}) \\ &= \phi^J (m_k - \bar{\sigma}^{2,J}) \\ &= \phi^J d_k. \end{aligned}$$

Thus, by iteration,

$$d_k = (\phi^J)^k d_0.$$

Since $m_0 = \sigma^2_{t+1}$, we have

$$d_0 = m_0 - \bar{\sigma}^{2,J} = \sigma^2_{t+1} - \bar{\sigma}^{2,J}.$$

Therefore,

$$d_k = (\phi^J)^k \big(\sigma^2_{t+1} - \bar{\sigma}^{2,J}\big).$$

Substituting back $d_k = m_k - \bar{\sigma}^{2,J}$ gives

$$m_k = \bar{\sigma}^{2,J} + (\phi^J)^k \big(\sigma^2_{t+1} - \bar{\sigma}^{2,J}\big).$$

Finally, for $k = 0$,

$$m_0 = \bar{\sigma}^{2,J} + (\phi^J)^0 \big(\sigma^2_{t+1} - \bar{\sigma}^{2,J}\big) = \sigma^2_{t+1}.$$

This verifies the solution. □

where $\bar{\sigma}^{2,J} = \omega^J/(1 - \phi^J)$ is the unconditional variance, which exists under the stationarity condition $\phi^J < 1$ imposed in calibration. This expression holds for $k \geq 0$, with $k = 0$ recovering the current variance σ^2_{t+1}. Expected future variance is thus a weighted average of the unconditional and current variance, with the weight on the deviation decaying geometrically at rate ϕ^J.

Step 3: Expected realized variance. To obtain expected realized variance, we average over the horizon. Because the variance process is Markov in σ^2, the conditional mean of future variance depends on $\mathcal{F}_t$ only through the state σ^2_{t+1}. The definition $RV_{t,T} = \frac{1}{\tau}\sum_{i=t+1}^{T} \sigma^2_i$ gives:

$$E^J[RV_{t,T} \mid \mathcal{F}_t] = \frac{1}{\tau}\sum_{j=0}^{\tau-1} E^J[\sigma^2_{t+1+j} \mid \mathcal{F}_t] = \bar{\sigma}^{2,J} + \frac{\sigma^2_{t+1} - \bar{\sigma}^{2,J}}{\tau}\sum_{j=0}^{\tau-1}(\phi^J)^j. \tag{17}$$

Evaluating the geometric sum $\sum_{j=0}^{\tau-1}(\phi^J)^j = (1 - (\phi^J)^\tau)/(1 - \phi^J)$ and defining the mean-reversion adjustment factor:

$$\kappa^J_\tau = \frac{1 - (\phi^J)^\tau}{\tau(1 - \phi^J)}, \tag{18}$$

yields the closed-form expression:

$$E^J[RV_{t,T} \mid \mathcal{F}_t] = \bar{\sigma}^{2,J}(1 - \kappa^J_\tau) + \kappa^J_\tau \sigma^2_{t+1}. \tag{19}$$

As $\tau \to \infty$, $\kappa_\tau^J \to 0$ and expected realized variance converges to the unconditional variance.

Step 4: VRP decomposition. Applying this expression to the physical measure P with $(\omega, \beta, \alpha, \gamma)$, the counterfactual $\tilde{Q}$ with $(\omega^*, \beta^*, \alpha^*, \gamma)$, and the risk-neutral measure Q with $(\omega^*, \beta^*, \alpha^*, \gamma^*)$ yields the variance risk premium decomposition. Note that $\tilde{Q}$ and Q share the same $(\omega^*, \beta^*, \alpha^*)$ but differ only in the asymmetry parameter, so:

$$VRP_{t,T}^{leverage} = E^Q[RV_{t,T} \mid \mathcal{F}_t] - E^{\tilde{Q}}[RV_{t,T} \mid \mathcal{F}_t] \tag{20}$$

$$= \left[\bar{\sigma}^{2,Q}(1 - \kappa_\tau^Q) + \kappa_\tau^Q \sigma_{t+1}^2\right] - \left[\bar{\sigma}^{2,\tilde{Q}}(1 - \kappa_\tau^{\tilde{Q}}) + \kappa_\tau^{\tilde{Q}} \sigma_{t+1}^2\right]. \tag{21}$$

The difference arises solely from how γ^* versus γ affects the unconditional variance $\bar{\sigma}^{2,J}$, the persistence ϕ^J, and the mean-reversion factor κ_τ^J.

This measures how much the market increases expected variance when moving from the counterfactual $\tilde{Q}$ (option-implied base dynamics with historical leverage) to the risk-neutral measure Q (option-implied leverage), i.e., the incremental price of downside-asymmetric variance risk embedded in γ^*.

A.5 Economic Magnitude Derivation Details

This section provides the full derivation chain underlying the back-of-the-envelope economic translation in Section 4.4. The goal is to map the DiD coefficient on the log leverage premium into an approximate dollar cost of downside protection per contract and per head. The exercise is an illustrative local translation anchored to representative characteristics from the sample, not an exact repricing of every observed option.

Step 1: DiD Coefficient to Variance Increment Define the leverage-premium ratio as

$$R \equiv \frac{E^{\mathbb{Q}}[RV]}{E^{\tilde{\mathbb{Q}}}[RV]}, \tag{22}$$

where $E^{\mathbb{Q}}[RV]$ is risk-neutral expected realized variance and $E^{\tilde{\mathbb{Q}}}[RV]$ is the counterfactual expected variance that retains historical asymmetry. The dependent variable in the DiD regression is $\log R$.

Let R_0 denote the baseline ratio before the fire. From Table 3, the sample-average log leverage premium for live cattle regular options is approximately 0.22, so $R_0 = e^{0.22} \approx 1.246$. The preferred Shutdown DiD estimate $\hat{\beta}_3 = 0.14$ says that the fire raised $\log R$ by 0.14 log points for live cattle relative to corn. In levels, this means the ratio is scaled by $e^{0.14} \approx 1.150$, so the post-shock ratio is

$$R_1 = R_0 \cdot e^{0.14}. \tag{23}$$

Converting back to expected variance levels, the pre-fire risk-neutral variance is $E^{\mathbb{Q}}[RV]_{\text{pre}} = E^{\tilde{\mathbb{Q}}}[RV] \cdot R_0$ and the post-fire level is $E^{\mathbb{Q}}[RV]_{\text{post}} = E^{\tilde{\mathbb{Q}}}[RV] \cdot R_0 \cdot e^{0.14}$. The fire-induced increment is the difference:

$$\begin{aligned} \Delta E^{\mathbb{Q}}[RV] &= E^{\mathbb{Q}}[RV]_{\text{post}} - E^{\mathbb{Q}}[RV]_{\text{pre}} \\ &= E^{\tilde{\mathbb{Q}}}[RV] \cdot R_0 \cdot e^{0.14} - E^{\tilde{\mathbb{Q}}}[RV] \cdot R_0 \\ &= E^{\tilde{\mathbb{Q}}}[RV] \cdot R_0 \cdot (e^{0.14} - 1). \end{aligned} \tag{24}$$

Substituting $E^{\tilde{\mathbb{Q}}}[RV] \approx 6.92 \times 10^{-5}$ from Table 3, $R_0 \approx 1.246$, and $e^{0.14} - 1 \approx 0.150$:

$$\Delta E^{\mathbb{Q}}[RV] \approx 6.92 \times 10^{-5} \times 1.246 \times 0.150 \approx 1.29 \times 10^{-5}. \tag{25}$$

Annualizing ($\times 252$ trading days) gives $\Delta v \approx 0.0033$, where v denotes annualized implied variance.

In plain terms: the pre-fire risk-neutral variance level is $E^{\tilde{\mathbb{Q}}}[RV] \times R_0$; the DiD estimate says the fire raised that level by 15.0%; multiplying the two gives the absolute variance increment.

Step 2: Variance Increment to Implied Volatility For short-dated OTM options not too far from the money, Black-76 implied variance provides a reasonable local approximation to risk-neutral expected realized variance. We therefore treat Δv as an approximate increment to annualized Black-76 implied variance. Because the leverage premium operates through asymmetric volatility ($\gamma^* > \gamma$), the additional risk-neutral variance concentrates on the left tail of the return distribution, implying that OTM put implied volatilities likely rose by more than the average $\Delta\sigma$ computed here. The estimates in Steps 3 and 4 are therefore conservative for the OTM puts most relevant to hedging demand.

Convert the annualized variance increment Δv to an implied volatility increment $\Delta\sigma$. Let $f : v \mapsto \sigma = \sqrt{v}$. Taking the derivative:

$$f'(v) = \frac{d}{dv}\sqrt{v} = \frac{1}{2\sqrt{v}} = \frac{1}{2f(v)}$$

A first order Taylor approximation of f around a specific base point v_{pre} is

$$f(v_{\text{pre}} + \Delta v) \approx f(v_{\text{pre}}) + f'(v_{\text{pre}})\Delta v$$

Using the variance swap rate we can treat the Black-76 implied variance and model variance as interchangeable. Black-76 provides a reasonable local approximation to risk-neutral expected realized variance when you have short-dated not too far OTM puts $\sigma^2 \approx E^Q[RV]_{\text{annualized}}$ such that Δv can be treated as an increment to the empirical $\bar{\sigma}^2$ in the Taylor series expansion.

By construction $\sigma_{\text{post}} \approx f(v_{\text{pre}}) + f'(v_{\text{pre}})\Delta v$ where $v_{\text{post}} = v_{\text{pre}} + \Delta v$ and f maps variance to volatility, so $f(v_{\text{post}}) = \sigma_{\text{post}}$.

Using Black-76 implied volatility from Table 1 $\bar{\sigma} \equiv f(v_{\text{pre}})$ and $f'(v_{\text{pre}}) = \frac{1}{2\bar{\sigma}}$. So rewriting we have that

$$\sigma_{\text{post}} \approx \bar{\sigma} + \frac{1}{2\bar{\sigma}}\Delta v$$

Subtracting $\bar{\sigma}$ from both sides yields

$$\sigma_{\text{post}} - \bar{\sigma} \approx \frac{\Delta v}{2\bar{\sigma}}$$

Now define $\Delta\sigma \equiv \sigma_{\text{post}} - \bar{\sigma}$ since this is the fire-induce bump in implied volatility. Therefore we have that:

$$\Delta\sigma \approx \frac{\Delta v}{2\bar{\sigma}}. \tag{26}$$

Using $\Delta v \approx 0.0033$ and $\bar{\sigma} \approx 0.184$ (the average annualized implied volatility for OTM live cattle puts in the $[0.85, 1.00)$ moneyness range from Table 1):

$$\Delta\sigma \approx \frac{0.0033}{2 \times 0.184} \approx 0.009. \tag{27}$$

This yields approximately 0.9 percentage points of additional implied volatility attributable to the repriced leverage effect. The linearization requires Δv to be small relative to $\bar{\sigma}^2$. Here $\Delta v/\bar{\sigma}^2 \approx 0.0033/0.034 \approx 0.10$, so the first-order approximation is reasonably accurate for our purposes.

Step 3: Implied Volatility to Option Cost The Black-76 model for a European put on a futures contract with price F, strike K, time to expiration τ, risk-free rate r, and implied volatility σ gives price

$$P = e^{-r\tau}\left[K\,\Phi(-d_2) - F\,\Phi(-d_1)\right], \tag{28}$$

where $\Phi(\cdot)$ is the standard normal CDF,

$$d_1 = \frac{\ln(F/K) + \frac{1}{2}\sigma^2\tau}{\sigma\sqrt{\tau}}, \qquad d_2 = d_1 - \sigma\sqrt{\tau}. \tag{29}$$

The sensitivity of the option price to implied volatility is vega:

$$\mathcal{V} = \frac{\partial P}{\partial \sigma} = F\, e^{-r\tau} \sqrt{\tau}\, \phi(d_1), \tag{30}$$

where $\phi(\cdot)$ is the standard normal PDF. This gives the price change in cents/cwt per one-unit change in σ; dividing by 100 converts it to a one-percentage-point change in implied volatility. To convert to dollars per contract, multiply by 400 cwt (one live cattle contract covers 40,000 lbs).

Evaluated at representative pre-fire contract characteristics, this local vega approximation converts the implied-volatility increment into a dollar premium effect. For a representative OTM put with $F = 110$ \$/cwt, $\sigma = 0.184$, $\tau = 45/252 \approx 0.179$, and $r \approx 0.02$: at $K/F = 0.95$ ($K = 104.5$), $d_1 \approx 0.70$ and $\phi(0.70) \approx 0.312$, giving $\mathcal{V} \approx 110 \times 0.996 \times 0.423 \times 0.312 \approx 14.5$ ¢/cwt per unit σ, or approximately \$58 per contract per percentage point. At $K/F = 0.97$ ($K = 106.7$), $d_1 \approx 0.47$ and $\phi(0.47) \approx 0.357$, giving $\mathcal{V} \approx 110 \times 0.996 \times 0.423 \times 0.357 \approx 16.6$ ¢/cwt per unit σ, or approximately \$68 per contract per percentage point.

Applied to a $\Delta\sigma \approx 0.9$ percentage-point increase, the local pricing effect is approximately \$52–\$61 per contract for representative puts in this strike range. Using somewhat lower-vega contracts within the broader OTM region yields a slightly wider back-of-the-envelope range of roughly \$50–\$60 per contract.

Step 4: Per-Head Cost One live cattle futures contract covers 40,000 lbs. At a market weight of approximately 1,300 lbs per finished animal, one contract corresponds to roughly $40{,}000/1{,}300 \approx 31$ head. The implied increase in per-head hedging cost is therefore:

$$\Delta P_{\text{head}} \;\approx\; \frac{[50,\,60]}{31} \;\approx\; \$1.60\text{–}\$1.90 \text{ per head.} \tag{31}$$

These calculations are intended to illustrate economic magnitude using representative contract inputs, not to recover the exact repricing of each option in the sample.

References

Barone-Adesi, G., Engle, R. F., & Mancini, L. (2008). A GARCH option pricing model with filtered historical simulation. *Review of Financial Studies*, 21(3), 1223–1258. https://doi.org/10.1093/rfs/hhn031

Carr, P., & Wu, L. (2009). Variance risk premiums. *Review of Financial Studies*, 22(3), 1311–1341. https://doi.org/10.1093/rfs/hhn038

Duan, J. C., & Simonato, J. G. (1998). Empirical martingale simulation for asset prices. *Management Science*, 44(9), 1218–1233. https://doi.org/10.1287/mnsc.44.9.1218

Glosten, L. R., Jagannathan, R., & Runkle, D. E. (1993). On the relation between the expected value and the volatility of the nominal excess return on stocks. *The Journal of Finance*, 48(5), 1779–1801. https://doi.org/10.1111/j.1540-6261.1993.tb05128.x

Nelder, J. A., & Mead, R. (1965). A simplex method for function minimization. *The Computer Journal*, 7(4), 308–313.

Zhu, C., Byrd, R. H., Lu, P., & Nocedal, J. (1997). Algorithm 778: L-BFGS-B: Fortran subroutines for large-scale bound-constrained optimization. *ACM Transactions on Mathematical Software*, 23(4), 550–560. https://doi.org/10.1145/279232.279236

B Appendix Supplementary Tables and Figures

Figure B.1: Daily Settlement Prices

Note: Each panel displays the daily settlement prices for the first five nearby futures contracts for the indicated commodity from 2006 through 2021. The data are sourced from Bloomberg continuous contract files. Contracts are plotted using their respective ticker prefixes (e.g., ZC1 to ZC5 for Corn), and reflect calendar-rolled series based on Bloomberg's methodology.

Figure B.2: Daily Returns, Conditional Volatility, and Standardized Innovations

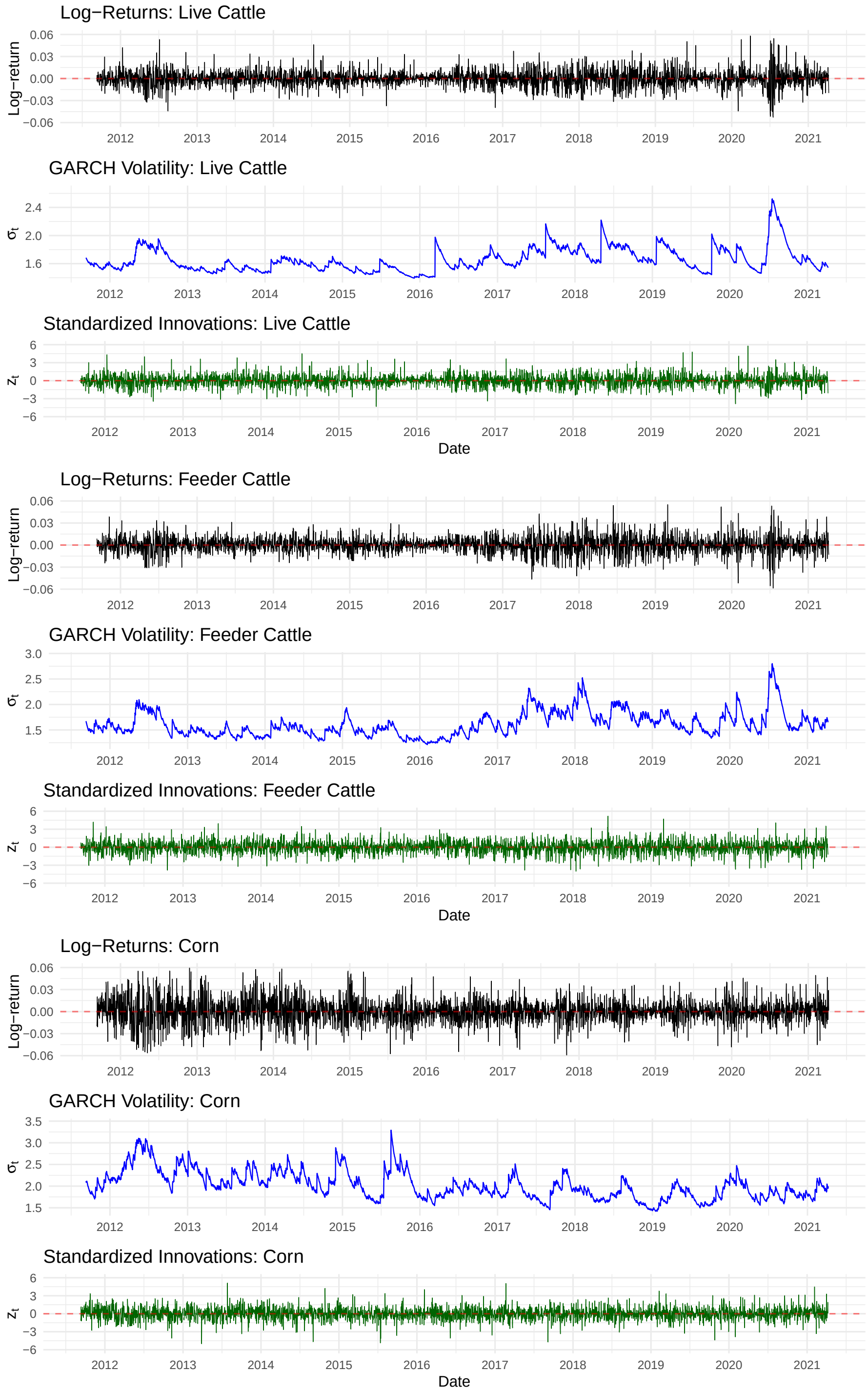

Note: Each panel displays daily log-returns, annualized GJR-GARCH conditional volatilities, and standardized innovations for live cattle, feeder cattle, and corn. The GARCH models are estimated using 3,500-day rolling windows ending at the representative calibration date. For each commodity, log-returns are shown in the top panel, GARCH-implied volatilities in the middle, and standardized innovations in the bottom panel.

Figure B.3: Hedging Pressure Time Series

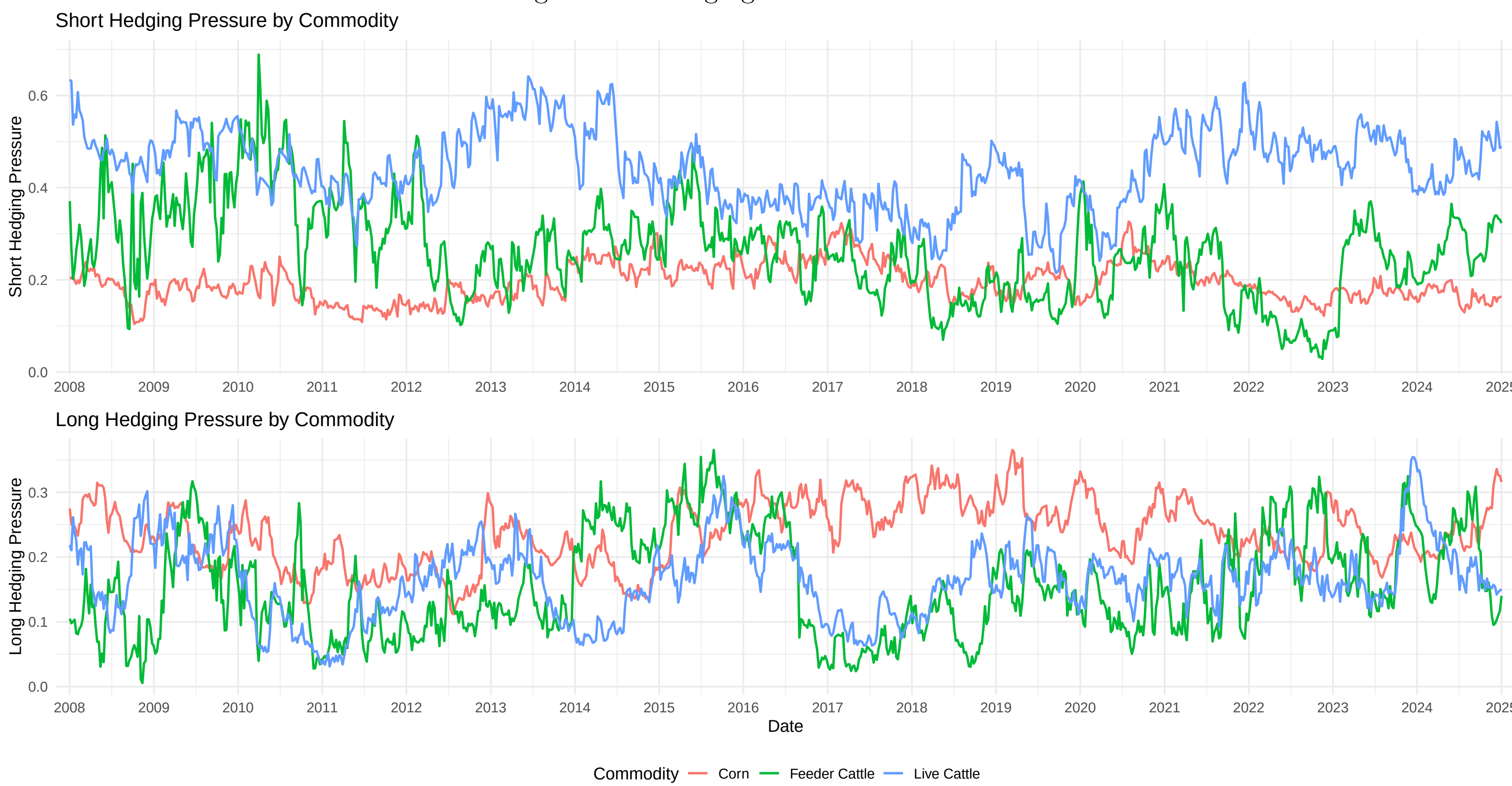

Note: This figure displays short and long term hedging pressure for agricultural commodities from 2008 to 2025. Hedging pressure measures the proportion of options open interest held by commercial hedgers (producers/merchants/processors/users) relative to total options open interest, calculated from the CFTC's weekly Commitment of Traders reports. Short hedging pressure (top panel) represents commercials' demand for protective put options to manage downside price risk, while long hedging pressure (bottom panel) represents their demand for call options to manage upside price risk. Higher values indicate stronger hedging demand from commercial participants. These series are used to construct the hedging-pressure controls included in the +T+HP and Full specifications in Section 4.

Table B.1: Agricultural Futures and Options Contract Expiry Rules

Commodity	Type	JAN	FEB	MAR	APR	MAY	JUN	JUL	AUG	SEP	OCT	NOV	DEC
Corn	Futures	–	–	15th	–	15th	–	15th	–	15th	–	–	15th
	Options	–	Last Fri*	–	Last Fri*	–	Last Fri*	15th	Last Fri*	–	–	Last Fri*	–
Feeder Cattle	Futures	Last Thurs*	–	Last Thurs*	Last Thurs*	Last Thurs*	–	–	Last Thurs*	Last Thurs*	Last Thurs*	Last Thurs*	–
	Options	Last Thurs*	–	Last Thurs*	Last Thurs*	Last Thurs*	–	–	Last Thurs*	Last Thurs*	Last Thurs*	Last Thurs*	–
Live Cattle	Futures	–	Last Day	–	Last Day	–	Last Day	–	Last Day	–	Last Day	–	Last Day
	Options	–	1st Fri	–	1st Fri	–	1st Fri	–	1st Fri	–	1st Fri	–	1st Fri

Note: Futures rules: Trading terminates on the business day prior to the 15th day of the contract month (Corn). Trading terminates on the last Thursday of the contract month. If the last Thursday of the contract month or any of the 4 prior weekdays is not a business day, trading terminates on the prior Thursday that is a business day and is preceded by a business day. Nov: Trading terminates on the Thursday prior to Thanksgiving Day (Feeder Cattle). Trading terminates at 12:00 Noon CT on the last business day of the contract month (Live Cattle). Options rules: Trading terminates on Friday which precedes, by at least 2 business days, the last business day of the month prior to the contract month (Corn). Trading terminates on the last Thursday of the contract month. If the last Thursday of the contract month or any of the 4 prior weekdays is not a business day, trading terminates on the prior Thursday that is a business day and is preceded by a business day. Nov: Trading terminates on the Thursday prior to Thanksgiving Day. (Feeder Cattle). Trading terminates at 1:00 p.m. CT on the first Friday of the contract month (Live Cattle). The "contract month" vocabulary in the options rules means "futures contract month expiry". Settlement rules are based on the nature of the contracts (i.e., deliverable, Corn, Live Cattle, and cash settled, Feeder Cattle).These expiry rules determine the option-maturity selection procedure described in Section 3.1.

Table B.2: Control Validity: $\gamma^* - \gamma$ Across Window Lengths

		1 Week		2 Weeks		3 Weeks		4 Weeks	
Option Type	Commodity	Δ	p	Δ	p	Δ	p	Δ	p
Regular	LC	0.3083	0.018	0.2303	0.007	0.1609	0.013	0.1626	0.014
	FC	0.1230	0.103	0.2728	0.003	0.1458	0.027	0.0601	0.335
	ZC	0.0148	0.870	-0.0010	0.983	0.0077	0.837	0.0075	0.803
Serial	LC	0.3871	0.020	0.2286	0.012	0.1617	0.009	0.1196	0.014
	FC	0.0107	0.937	-0.0033	0.961	-0.0246	0.620	-0.0040	0.921
	ZC	-0.0005	0.102	0.0029	0.233	0.0097	0.045	0.0115	0.010

Note: Table reports pre–post mean changes and two-sided Welch unequal-variance t-test p-values for $\gamma^* - \gamma$ across window lengths.

Table B.3: Control Validity: Log Leverage Premium Across Window Lengths

		1 Week		2 Weeks		3 Weeks		4 Weeks	
Option Type	Commodity	Δ	p	Δ	p	Δ	p	Δ	p
Regular	LC	0.2124	0.100	0.1889	0.046	0.1163	0.056	0.1213	0.060
	FC	0.0986	0.090	0.2625	0.001	0.1329	0.025	0.0447	0.413
	ZC	0.0136	0.827	-0.0002	0.995	0.0065	0.806	0.0034	0.877
Serial	LC	0.6611	0.074	0.3231	0.027	0.2008	0.016	0.1254	0.034
	FC	0.0088	0.964	-0.0211	0.843	-0.0602	0.434	-0.0287	0.661
	ZC	0.0392	0.062	0.0187	0.441	0.0486	0.014	0.0606	0.001

Note: Table reports pre–post mean changes and two-sided Welch unequal variance t-test p-values for the log leverage premium across alternative window lengths.